Molecular Biology of the Cell
Vol. 20, 4856–4870, November 15, 2009

Immobilization of the Glycosylphosphatidylinositol-anchored Gas1 Protein into the Chitin Ring and Septum Is Required for Proper Morphogenesis in Yeast

Eleonora Rolli,*†‡ Enrico Ragni,*† Julia Calderon,* Silvia Porello,§ Umberto Fascio,‖ and Laura Popolo*

*Dipartimento di Scienze Biomolecolari e Biotecnologie and ‖Centro Interdipartimentale Microscopia Avanzata, Università degli Studi di Milano, 20133 Milano, Italy; and §Department of Chemistry, Ursinus College, Collegeville, PA 19426

Submitted December 1, 2008; Revised September 8, 2009; Accepted September 17, 2009
Monitoring Editor: Howard Riezman

Gas1p is a glucan-elongase that plays a crucial role in yeast morphogenesis. It is predominantly anchored to the plasma membrane through a glycosylphosphatidylinositol, but a fraction was also found covalently bound to the cell wall. We have used fusions with the green fluorescent protein or red fluorescent protein (RFP) to determine its localization. Gas1p was present in microdomains of the plasma membrane, at the mother-bud neck and in the bud scars. By exploiting the instability of RFP-Gas1p, we identified mobile and immobile pools of Gas1p. Moreover, in *chs3*Δ cells the chitin ring and the cross-linked Gas1p were missing, but this unveiled an additional unexpected localization of Gas1p along the septum line in cells at cytokinesis. Localization of Gas1p was also perturbed in a *chs2*Δ mutant where a remedial septum is produced. Phenotypic analysis of cells expressing a fusion of Gas1p to a transmembrane domain unmasked new roles of the cell wall-bound Gas1p in the maintenance of the bud neck size and in cell separation. We present evidence that Crh1p and Crh2p are required for tethering Gas1p to the chitin ring and bud scar. These results reveal a new mechanism of protein immobilization at specific sites of the cell envelope.

INTRODUCTION

In yeast, morphogenesis and cell wall biogenesis are two tightly linked and mutually dependent processes that are responsible for the changes of cell shape occurring at different stages of the life cycle. The cell wall results from the cross-linking of various polymers that forms a fabric strong enough to counteract the high turgor pressure of yeast cells. In the budding yeast *Saccharomyces cerevisiae*, the network consists of an ordered thread of chitin, β(1,3)/(1,6)-glucans and mannoproteins (constituting ~1–2, 60, and 40–45% of the cell wall dry weight, respectively) (Klis *et al*., 2006; Lesage and Bussey, 2006). Cross-linking enzymes act on β(1,3)-glucan chains extruded by the plasma membrane β(1,3)-glucan synthases Fks1 and Fks2 and β(1,6)-glucan chains (the site of whose synthesis may be the cell surface or along the secretory pathway) (Montijn *et al*., 1999; Lesage *et al*., 2004; Lesage and Bussey, 2006). Moreover, surface mannoproteins and chitin molecules extruded by chitin synthases are also substrates of the cross-linking process.

This article was published online ahead of print in *MBC in Press* (http://www.molbiolcell.org/cgi/doi/10.1091/mbc.E08–11–1155) on September 30, 2009.

† These authors equally contributed to this work.

‡ Present address: Dipartimento di Scienze e Tecnologie Agroalimentari e Microbiologiche (DiSTAM) Università degli Studi di Milano, 20133 Milano, Italy.

Address correspondence to: Laura Popolo (laura.popolo@unimi.it).

Abbreviations used: α-F, α-factor; CF, calcofluor white.

Chitin synthesis is catalyzed by three distinct chitin synthases (CSI, II, and III), which use Chs1p, Chs2p, and Chs3p as the catalytic subunit, and is crucial for yeast morphogenesis. Most of the chitin in the cell is produced by Chs3p and is localized in the "chitin ring," which forms in the cell wall shortly before bud emergence, whereas only a tiny amount is deposited in the lateral cell walls (Shaw *et al*., 1991). Chs2p is required for the synthesis of the primary septum (~10% of total chitin), a thin disk of chitin that forms centripetally within the confines of the chitin ring at the onset of cytokinesis. Deposition of chitin by Chs2p is concomitant with the constriction of the actomyosin ring (for review, see Cabib, 2004). After cell separation the chitin ring remains on the mother cell as the crater-like "bud scar." Finally, Chs1p has a repair function preventing lysis at the birth scar due to excessive hydrolysis of the septum by chitinase. The contribution of Chs1p to the chitin content of a cell is negligible (Cabib *et al*., 1989).

The chitin ring delimits the neck and its presence contributes to preventing growth at the mother-daughter neck region. In fact, a constriction of constant diameter is maintained during the budded phase of the cell cycle (Cabib, 2004). Both septins and chitin ring are known to cooperate in ensuring the integrity of the neck. Defects in either of these elements result in a dramatic widening of the neck diameter and lethality (Schmidt *et al*., 2003; Cabib, 2004).

To date, only a few classes of extracellular enzymes have been identified as cell wall cross-linking/remodeling enzymes. One of them is the Gas protein family that is composed by five members, Gas1 to Gas5 (Ragni *et al*., 2007b). Gas1p is expressed during vegetative growth together with Gas5p, which seems to play an auxiliary role. Gas2p and

Gas4p are specifically expressed during meiosis and are essential for spore wall formation (Ragni *et al*., 2007a). Gas3p function is still unknown. Genes encoding Gas homologous proteins were found in all yeast and fungal species so far sequenced (Ragni *et al*., 2007b).

Gas proteins are modified by GPI, a glycolipid moiety bound to the C-terminal end that anchors the protein to the outer leaflet of the lipid bilayer in the plasma membrane. GPI confers lateral mobility in the lipid environment to the proteins (Malinska *et al*., 2004) and promotes association with specific membrane microdomains known as "lipid rafts." These microdomains are enriched in sphingolipids and ergosterol. Gas1p was recovered in the detergent-resistant membranes (DRMs), also named detergent-insoluble glycolipid-enriched complexes, which is indicative of an association with lipid rafts (Bagnat *et al*., 2000; Simons and Vaz, 2004; Aronova *et al*., 2007).

In yeast, the protein modification by GPI attachment has an additional role compared with animals and plants. At the cell surface, GPI-containing proteins can undergo a transglycosylase reaction whereby they are cleaved inside the glycan moiety of the GPI and linked to the glucan network with consequent release of the remaining glucosamine-phosphatydylinositol (GlcN-PI) moiety of the GPI (Kollar *et al*., 1997). This class of proteins is called GPI-cell wall proteins (GPI-CWPs, where GPI indicates a GPI remnant) and is the most abundant in the cell wall. To date the molecular mechanism of this process is still obscure. The putative mannosidases Dfg5p and Dcw1p were proposed as candidate catalysts of the transglycosylase reaction (Kitagaki *et al*., 2002).

The nonreducing end of β(1-3)-glucan is an acceptor site for the attachment of chitin, PIR-proteins or β(1-6)-glucan to which the GPI-CWPs are linked (for a review see Klis *et al*., 2006). Short side branches of the β(1-6)-glucan provide a further attachment site for the reducing end of chitin. Thus, β(1-6)-glucan is a core component of the cell wall to which GPI-CWPs, chitin and β(1-3)-glucan can be linked (Kollar *et al*., 1997). The formation of the cross-links occurs by transglycosylation reactions because small energy-rich molecules are unavailable outside the cell.

Recently, it has been demonstrated that the GPI-containing proteins Crh1 and Crh2 are responsible of the linkage of chitin to the side branches of β(1-6)glucan (Cabib *et al*., 2008). These enzymes are localized to the bud neck, bud scar and in minor amount all over the cell periphery. Interestingly, the activity of transferring chitin on β(1,6)-glucan is high in the bud scars and may be involved in tethering mannoproteins at these sites (Rodriguez-Pena *et al*., 2002; Cabib *et al*., 2007, 2008).

Gas1p acts as a β(1,3)-glucan elongase in in vitro assays (Mouyna *et al*., 2000). Its presumable in vivo role is to incorporate new β(1,3)-glucan chains into the preexisting cell wall and also create anchoring sites for other cell wall components (Kollar *et al*., 1995; Mouyna *et al*., 2000). Gas1p is predominantly located in the plasma membrane, but it is also linked to cell wall β(1,3)-glucan (De Sampaio *et al*., 1999). A comprehensive mass spectrometry analysis of the cell wall proteome revealed that Gas1, Gas3, and Gas5 proteins are covalently cross-linked to the glycan network (Yin *et al*., 2005). Besides Gas proteins, other GPI-CWPs with putative cell wall cross-linking activity were recovered in the cell wall proteome, notably Crh1p and Crh2p. Because it is still unclear whether anchoring of GPI-mannoproteins to the cell wall is simply a consequence of some leakiness in the mechanism of plasma membrane retention or a specific destination of the protein (Yin *et al*., 2005), we have investigated the cellular location of Gas1p. We report novel and unexpected locations of Gas1p and show that anchoring of Gas1p to specific cell wall destinations contributes to yeast morphogenesis.

MATERIALS AND METHODS

Yeast Strains and Growth Conditions

The strains used are listed in Table 1. Cells were grown in batch at 30°C in YPD (1% yeast extract, 2% Bacto-peptone, and 2% glucose) or in synthetic dextrose minimal medium (SD) (Difco yeast nitrogen base without amino acids [Difco, Detroit, MI] at 6.7 g/l and 2% glucose) to which amino acids and uracil were added to a concentration of 50 and adenine to 100 mg/l. For solid media, 2% agar was added to YPD or SD media (YPDA and SDA). When required, YPD was buffered at pH 6.5 with 10 g/l 2-(*N*-morpholino)ethanesulfonic acid (MES). Growth was monitored as the increase in OD_{450}. Duplication time (T_d) was calculated using the equation $T_d = \ln 2/K$, where K, the growth rate constant, is the slope of the line obtained by linear regression on a semilogarithmic plot of the OD values. The growth rate, μ (h^{-1}) was calculated as $1/T_d$.

Cloning of GAS1 Gene from SK1 Strain

The *GAS1* gene, encompassing 400 base pairs upstream and 300 base pairs downstream the coding sequence, was amplified by polymerase chain reaction (PCR) from genomic DNA of AN120 strain using the primers (restriction sites underlined) GAS1-PROM-SmaI GCATATTCGACTGACCCGGGGCCAGCCCTGGCTATTCTTT and GAS1-TERM-BamHI ATCGTCGGGCTCGGATCCTATGGAGAAAGTACATAAATG and Expand HiFidelity DNA polymerase (Roche Diagnostics, Indianapolis, IN). The amplified fragment was cloned in pCRII TA-TOPO cloning vector (Invitrogen, Carlsbad, CA) to create plasmid pER-1. Sequence verification was carried out by sequencing both strands of plasmids extracted from three transformants. Single-nucleotide polymorphisms were found, in agreement with the reported polymorphism of the SK1 strain compared with S288c (Primig *et al*., 2000). In the *GAS1* 5′-flanking region, a T insertion was present at nucleotide −49 from the initiation codon (the A of ATG was defined as nucleotide 1). In the open reading frame, C-to-T and G-to-A transitions, T-to-A transversion, and A-to G and G-to-A transitions were found at nucleotides 51, 156, 822, 855, and 1374, respectively, but these changes were silent. A T-to-A transversion and an A-to-G transition, respectively, at nucleotides 822 and 932, cause the following amino acid substitutions: T211 to A and N311 to S. In the 3′-flanking region, a C-to-G transition was present at nucleotide 1691. Yeast plasmids pYER-1 and pRS-1 were obtained by cloning the SmaI-BamHI fragment from pER-1 into the like sites of the YEp24 and pRS416 vectors.

Construction of S. cerevisiae Strains and GAS1p-Green Fluorescent Protein (GFP) Fusion

The inactivation of *GAS1* gene in AN120 strain was performed using short-homology polymerase chain reaction (PCR) gene targeting. Plasmid pFA6a-KanMX2, containing the module KanMX2 with the *kanR* gene, was used to amplify a PCR fragment used to inactivate *GAS1* (GAS1KFOR, 5′-TGGTATTCCTCATACAGCCTGCGCGGTTTATTAGTAAAATACCCGATAATCCTCGAGGTTGATATCAAGCTTGCCTCG-3′; GAS1KREV, 5′-CTCCGTTTGGAGTTGGTGGTAATTCTGTTGCAGCGGACCAGTACTTACCAGTAGCTGGACGTCGACACTGGATGGCGG-3′—sequences annealing to *kanR* gene are underlined). The 1556-base pair PCR fragment, harboring ends complementary to the −248 to −189 and +1043 to +1102 from the AUG start codon of *GAS1*, was used to transform the haploid strains AN117-16D and AN117-4B (Table 1). *S. cerevisiae* cells were transformed using the S.C. EasyComp transformation kit (Invitrogen). Genomic DNA isolated from the transformant clones was subjected to five different PCR diagnostic tests to verify correct integration. The primers used were AEV25, 5′-AGTTTTCGTGCCGCAAACGT-3′; AEV26, 5′-AGTTCCGGAACCCAAATCAA-3′; GAS1ORF, 5′-AACACAGATGCATCTGCT-3′; GAS1OREV, 5′-AGCAGATGCATCTGTGTT-3′; KANMX2REV, 5′-GTAATGGCTGGCCTGTTG-3′; and KANMX2, 5′-CAACAGGCCAGCCATTAC-3′). The haploid strains carrying the *gas1*Δ mutation were crossed to generate *gas1*Δ/*gas1*Δ (ER320) null diploid. The lack of Gas1p was confirmed by immunoblotting.

Strain JC9 was constructed by transforming WAH cells (*gas1*Δ) with integrative plasmid pMF608, a kind gift of Prof. Y. Jigami (AIST, Tokyo, Japan). Plasmid pMF608 harbors an mRFP-*GAS1* fusion under the control of the natural *GAS1* promoter. The N-terminal sequence of the encoded hybrid protein is *MLFKSLSKLATAAAFFAGVATA* ↓ *D*TRAS**ASSE**—where the signal peptide of Gas1p is in italics, the amino acids of the linker are underlined, the first amino acids of monomeric red fluorescent protein (mRFP) are in bold, and the arrow indicates the cleavage site for leader peptidase. Plasmid pMF608 was linearized by digestion with BfrI for targeting into the *LEU2* locus. Leu^+ transformants were analyzed for the presence of the fluorescent protein and JC9 strain was analyzed in more detail (Table 1).

The GFP module was amplified by PCR from plasmid pFA6a-GFP(S65T)-KanMX6 with the following primers containing a BseAI restriction site

Table 1. Strains used in this work

Strain	Genotype	Relevant genotype	Source
W303-1A	*Mata ade2-1 his3-11,15 trp1-1 ura3-1 leu2-3,112 can1-100*	*Parental strain*	CNRS, France
W303-1B	*Matα ade2-1 his3-11,15 trp1-1 ura3-1 leu2-3,112 can1-100*	*Parental strain*	CNRS, France
*chs3*Δ	*MATα chs3::LEU2 ade2-1 his3-11,15 trp1-1 ura3-1 leu2-3,112 can1-100*	*chs3*Δ	A. Duran, Universidad de Salamanca, Spain
WB2d	W303-1B *gas1::LEU2*	*gas1*Δ	Vai *et al*. (1991)
WAH	W303-1A *gas1::HIS3*	*gas1*Δ	Vai *et al*. (1991)
JC9	WAH *leu2*::pMF608 mRFP-*GAS1 LEU2*	*gas1*Δ *mRFP-GAS1*	This work
JC10	WAH *leu2*::pMF608TM mRFP-*GAS1-MID2 LEU2*	*gas1*Δ *mRFP-GAS1-MID2*	This work
W303-*GAS1*-GFP	W303-1B [pRS424-*GAS1-GFP 2 μ TRP1*]	*GAS1-GFP*	This work
WB2d-GAS1-GFP	WB2d [pRS424-*GAS1-GFP 2 μ TRP1*]	*gas1*Δ *GAS1-GFP*	This work
*chs3*Δ-GAS1-GFP	*chs3*Δ [pRS424-*GAS1-GFP 2 μ TRP1*]	*chs3*Δ *GAS1-GFP*	This work
AN117-4B	*MATα ura3 leu2 his3 trp1 lys2 arg4 ho::LYS2 rme1::LEU2*	*Parental strain*	A. Neiman, Stony Brook University
AN117-16D	*MATa ura3 leu2 his3 trp1 lys2 ho::LYS2*	*Parental strain*	A. Neiman
AN120	*(Cross AN117-4B x AN117-16D) MATa/α ura3/ura3 leu2/leu2 trp1/trp1 his3/his3 lys2/lys2 arg4/ARG4 ho::LYS2/ho::LYS2 rme1::LEU2/RME1*	*Parental strain*	Ragni *et al*. (2007a)
AN262	AN120 *and chs3::HIS5/chs3::HIS5*	*chs3*Δ	A. Neiman
ER310	AN120 [YEp24 *2m URA3*]		Ragni *et al*. (2007a)
ER320	AN120 and *gas1::KanMX2/gas1::KanMX2*	*gas1*Δ	This work
ER332	ER320 [pRS416 *CEN URA3*]	*gas1*Δ	This work
ER333	ER320 [YEp24]	*gas1*Δ	This work
ER334	ER320 [pRS416-*GAS1-URA3 CEN*]		This work
ER335	ER320 [YEp24-*GAS1*]		This work
ER336	ER320 [pRS416-*GAS1-GFP URA3 CEN*]	*gas1*Δ GAS1-GFP	This work
ER337	ER320 [YEp24-*GAS1-GFP*]	*gas1*Δ GAS1-GFP	This work
ER338	AN120 [pRS416]		This work
ER339	AN120 [pRS416-*GAS1*]		This work
ER340	AN120 [YEp24-*GAS1*]		This work
ER341	AN120 [pRS416-*GAS1-GFP*]	*GAS1-GFP*	This work
ER342	AN120 [YEp24-*GAS1-GFP*]	*GAS1-GFP*	This work
ER343	AN262 [pRS416-*GAS1-GFP*]	*chs3*Δ *GAS1-GFP*	This work
ER344	AN262 [YEp24-*GAS1-GFP*]	*chs3*Δ *GAS1-GFP*	This work
YPH499	*MATa ura3-52 leu2-Δ1 his3*Δ200 *trp1-Δ63 lys2-801 ade2-101*	*Parental strain*	E. Cabib, NIH
ECY46-1-8D	YPH499 *chs1::HIS3*	*chs1*Δ	E. Cabib, NIH
YMS11	YPH499 *chs2::TRP1*	*chs2*Δ	E. Cabib, NIH
ECY46-4-1B	YPH499 *chs3::LEU2*	*chs3*Δ	E. Cabib, NIH
CER1	YPH499 *gas1::LEU2*	*gas1*Δ	This work
CER2	YPH499 *chs1::HIS3 gas1::LEU2*	*chs1*Δ *gas1*Δ	This work
CER3	CER1 [YEp24-*GAS1-GFP*]	*gas1*Δ *GAS1-GFP*	This work
CER4	CER2 [YEp24-*GAS1-GFP*]	*chs1*Δ *gas1*Δ GAS1-GFP	This work
CER5	YMS11 [YEp24-*GAS1-GFP*]	*chs2*Δ *GAS1-GFP*	This work
BY4742	*MATα his3Δ1 leu2*Δ0 *ura3*Δ0 *lys2*Δ0	*Parental strain*	Euroscarf
TG208	BY4742 *gas1::LEU2*	*gas1*Δ	This work
Y14895	BY4742 *dcw1::KanMX4*	*dcw1*Δ	Euroscraf
Y10824	BY4742 *dfg5::KanMX4*	*dfg5*Δ	Euroscarf
ER369	Y14895 *gas1::LEU2*	*dcw1*Δ *gas1*Δ	This work
ER370	Y10824 *gas1::LEU2*	*dfg5*Δ *gas1*Δ	This work
ER371	TG208 [YEp24-*GAS1-GFP*]	*gas1*Δ *GAS1-GFP*	This work
ER372	ER369 [YEp24-*GAS1-GFP*]	*dcw1*Δ *gas1*Δ *GAS1-GFP*	This work
ER373	ER370 [YEp24-*GAS1-GFP*]	*dfg5*Δ *gas1*Δ *GAS1-GFP*	This work
BY4741	*MATa his3*Δ1 *leu2*Δ0 *ura3*Δ0 *met15*Δ0	*Parental strain*	Euroscarf
GRA006	BY4741 *crh2::HIS3*	*crh2*Δ	Cabib *et al*. (2007)
GRA007	BY4741 *crh1::hphMX4 crh2::HIS3*	*crh1*Δ *crh2*Δ	Cabib *et al*. (2007)
Y00897	BY4741 *gas1::KMX4*	*gas1*Δ	Cabib *et al*. (2007)
GR010	BY4741 *crh2::HIS3 gas1::KMX4*	*crh2*Δ *gas1*Δ	Cabib *et al*. (2007)
GR011	BY4741 *crh1::hphMX4 crh2::HIS3 gas1::KMX4*	*crh1*Δ *crh2*Δ *gas1*Δ	Cabib *et al*. (2007)
ER374	Y00897 [YEp24-*GAS1-GFP*]	*gas1*Δ *GAS1-GFP*	This work
ER375	GR010 [YEp24-*GAS1-GFP*]	*crh2*Δ *gas1*Δ *GAS1-GFP*	This work
ER376	GR011 [YEp24-*GAS1-GFP*]	*crh1*Δ *crh2*Δ *gas1*Δ *GAS1-GFP*	This work

(underlined): GAS1P-GFPup, ATATCCGACTGATCCGGAGGTGCCAGTAAAGGAGAAGAACTTTTCAC and GAS1P-GFPdown, ATCGTCCTCTATCCGGATTTGTATAGTTCATCCATG. The triplets encoding for Gly-Ala were introduced at the 5′ and 3′ flanking regions of the GFP coding sequence to act as spacers. The gel-purified PCR product was digested with BseAI and cloned in plasmid pER-1 (see above). Control digestions and sequencing were performed to verify the in-frame-fusion of the GFP module into the *GAS1* cds. The SmaI-BamHI fragment, containing the *GAS1-GFP* fusion gene, was cloned into the corresponding site of the YEp24 (multicopy) and pRS416 (CEN) vectors, generating YEp24-*GAS1*-GFP and pRS416-*GAS1*-GFP. These plasmids were used to transform AN120 and AN262 strains. The SmaI-BamHI fragment from YEp24-*GAS1*-GFP was cloned into a similarly digested pRS424 vector to give pRS424-*GAS1*-GFP. This plasmid was used to transform W303 and derived strains. The strains and their genotypes are listed in Table 1. The *GAS1* gene disruption in strains derived from YPH499 and BY4742 was performed as described previously (Vai *et al*., 1991).

Construction of the mRFP-GAS1-MID2 Fusion

The fusion gene was obtained by cloning in-frame the fragment of mRFP-*GAS1* ending at codon 484 of the *GAS1* open reading frame (ORF), with a DNA fragment of the cds (residues 213-376) of the *MID2* gene encompassing the transmembrane segment (residues 225-247), the cytosolic tail (residues 248-376), and the downstream transcription termination sequence. In a first PCR step, the fragment of *MID2* starting from nucleotide +637 to +1128 of the ORF and the 3′ downstream region from nucleotide +1129 to +1680

(being A of the starting ATG the nucleotide number +1) was amplified using the primers Mid2up (5′-ATATTCGACTGA**TCCGGA**TCCAAAAGTTCGG-GTCTTTC-3′) and Mid2down2 (5′-ACTCTGCTCTAC**TCCGGA**CTCCTTAT-GCTTCTACAC-3′). In each primer, a sequence recognized by BseAI was introduced (in bold). The amplified fragment of ~1.1 kbp was purified, BseAI digested, and ligated into the plasmid pMF608 previously linearized in the corresponding BseAI site at position +1453 of the *GAS1* ORF. The DNA plasmid from 20 generated clones was digested with NdeI to check for correct orientation. Two independent positive plasmids were named pMF608TM-15 and -16. The plasmids were linearized with BfrI and 10 μg of digested DNA were used to transform the WAH strain via integration in the *LEU2* locus to obtain JC10 strain (see Table 1).

α-Factor (α-F) Treatment

At a cell density of ~5 × 10^6 cells/ml (~0.3 $OD_{450\ nm}$), cells from strains JC9 and W303-1A, exponentially growing in YPD at 30°C, were collected by centrifugation, washed with fresh YPD, and suspended in YPD at the same cell density in the presence or absence of 20 μg/ml α-F (GenScript, Piscataway, NJ). At different time intervals from α-F addition, aliquots corresponding to 13, 20, or 50 OD_{450} were collected for the preparation of total extracts, for subcellular fractionation and cell wall purification, respectively.

Microscopy Analysis

Cells were routinely observed by phase-contrast microscopy and scored for budding by counting at least 200 cells after mild sonication. For fluorescence microscopy cells were either fixed or analyzed without fixation. In either case, cells were sonicated before being processed. Approximately 2 × 10^8 cells were fixed in 3.7% formaldehyde and 0.1 M K-phosphate, pH 6.5. After 30 min at room temperature, cells were filtered and resuspended in the same volume of a fixing buffer (3.7% formaldehyde and 0.1 M K-phosphate, pH 6.5). Cells were kept at 4°C for one or more days. Cells were collected by centrifugation at 6000 × *g* for 2 min, washed twice with phosphate-buffered saline (PBS), pH 7.4, at 4°C and left in PBS for 1 h in ice before examination at the microscope. For observation without fixation, cells were collected by centrifugation, washed twice with PBS, and incubated at least 15 min for Gas1p-GFP and 1 h for mRFP-Gas1p on ice before being examined under the microscope. If required, 8.3 μg/ml 4,6-diamidine-phenylindole (DAPI) was added to the cells. Samples were then incubated for further 15 min at room temperature in the dark. Staining of chitin on unfixed cells was performed by using 2 μg/ml calcofluor (CF) white (Sigma-Aldrich, St. Louis, MO). Cells were stained for 3 min and washed once with PBS. In the α-F experiments, chitin staining was performed by adding 0.2 μg CF/ml culture during the last 10 min of growth before viewing the cells (Warenda and Konopka, 2002).

The cells were examined as wet mounts using a BX60 microscope (Olympus, Melville, NY) and a DC290 digital photo camera (Eastman Kodak , Rochester, NY) or an Eclipse 90i microscope (Nikon, Tokyo, Japan) equipped with epifluorescence, Nomarski optics, and a Hamamatsu ORCA-ER device camera (Nuhsbaum, McHenry, IL). For stack acquisition analysis, the z-distance was set to 0.4 μm. For confocal microscopy cells were examined using a TCS SP2 AOBS confocal laser-scanning microscope (Leica Microsystems, Heidelberg, Germany), equipped with Ar/Kr and He/Ne lasers and a PLAPO 63 oil immersion objective. Gas1p-GFP was excited with a laser line of λ = 488 nm, and the fluorescence was collected between 493 and 539 nm. mRFP-Gas1p was excited with a laser line of λ = 561 nm, and the fluorescence collected between 555 and 620 nm. DAPI or calcofluor were excited in the UV (λ = 364 nm) and the fluorescence was collected in the range 410 and 470 nm. A focal series of horizontal planes of section were assessed by sequential scanning of sample with 1.0-μm step size. Neck diameters were measured in differential interference contrast images by measuring the distance between the inner parts of the cell wall.

Calcofluor Sensitivity Assay

Five microliters from a concentrated suspension of cells (8 OD_{450}) and from 1:10 serial dilutions of it, were spotted on SDA or buffered SDA plates in the absence or presence of 2, 5, 10, and 20 μg of calcofluor white per milliliter. Growth was checked after 2 d at 30°C.

Flow Cytometry Analysis

Cells (1 OD_{450}) were mildly sonicated, collected by centrifugation, washed, and suspended in ice-cold 70% ethanol. Fixed cells were centrifuged, suspended in 0.5 ml of RNase A (1 mg/ml in 50 mM Tris-HCl, pH 7.5) and incubated for 2 h at 37°C. Cells were centrifuged and suspended in 0.5 ml of proteinase K (1 mg/ml in 50 mM Tris-HCl, pH 7.5). After 2 h at 42°C cells were collected, resuspended in the same volume of fluorescence-activated cell sorting (FACS) buffer (200 mM Tris-HCl, pH 7.5, 200 mM NaCl, and 78 mM $MgCl_2$), and then 100 μl was added to 1 ml Sytox Green 1× (1:5000 dilution in 50 mM Tris-HCl, pH 7.5; Invitrogen). The samples were sonicated for 10 s before analysis with a FACScan flow cytometer (BD Biosciences, San Jose, CA). We analyzed 10^4 cells for each sample, and the percentage of cells in G1, S ,and G2 + M phases was determined. The percentage of cells with a DNA content >2c was measured starting from the end of the G_2+M peak.

Extract Preparation, Precipitation of Protein from Medium, Electrophoresis, and Immunoblotting

For total extract, ~2 × 10^8 cells were collected by filtration, washed, quickly frozen in dry ice-acetone and stored at −20°C. The procedure for extract preparation in the presence of protease inhibitors (1 mM phenylmethylsulfonyl fluoride, a protease inhibitors cocktail [Roche Diagnostics] and 1 μg/ pepstatin A), and the determination of protein concentration was performed as described previously (Ragni *et al*., 2007a). For the analysis of Gas1p in the culture medium, cells were grown in YPD or in YPD-pH 6.5 and let grow to an OD_{450} of ~1.5. Culture supernatants were obtained by filtration of 27 ml of culture on nitrocellulose filters and proteins were precipitated in 10% trichloroacetic acid (TCA) in ice for at least 1 h. After 10-min centrifugation at 13,000 × *g*, the pellet was washed with 1 ml of ice-cold acetone and allowed to evaporate. The pellet was denatured in SDS-sample buffer [0.0625 M Tris-HCl, pH 6.8, 2.3% (wt/vol) SDS, 5% (vol/vol) β-mercaptoethanol, and 10% glycerol] and neutralized by addition of 1 M Tris. SDS-polyacrylamide gel electrophoresis (PAGE) and immunoblotting were performed as described previously (Gatti *et al*., 1994; Ragni *et al*., 2007a). Anti-Gas1p serum was obtained by immunizing rabbits with a soluble 6xHis-tagged form of Gas1p produced in *Pichia pastoris* (Ragni *et al*., 2007b). Immunization procedure was carried out by Areta International (Gerenzano, Varese, Italy). Anti-Gas1p serum was used at a dilution of 1:1000 in Tris-buffered saline (TBS)-bovine serum albumin (BSA) and 0.2% Tween 20. Monoclonal mouse anti-actin antibody, clone C4 (MP Biomedicals, Irvine, CA) was used at a dilution of 1:1000 in TBS-BSA, 0.1% Tween 20. Peroxidase-conjugated affinity purified $F(ab')_2$ fragment donkey anti-rabbit or anti-mouse immunoglobulin G were from The Jackson Laboratory (Bar Harbor, ME) and were diluted 1:10,000. Bound antibodies were revealed using the enhanced chemiluminescence Western blotting detection reagents (GE Healthcare, Chalfont St. Giles, Buckinghamshire, United Kingdom). Densitometric measurements of undersaturated films were performed using the program Scion Image (scion, Frederick, MD).

Subcellular Fractionation and Protein Extraction from Purified Cell Walls

For membrane separation, cells corresponding to 20 OD_{450} units were collected by centrifugation. The pellet was washed with distilled H_2O (dH_2O) and cells resuspended in 100 μl of 10 mM Tris-HCl, pH 7.5, supplemented with the protease inhibitors described above. Cells were mechanically broken in the presence of glass beads in a FastPrep 120 for three cycles or more at maximum speed until full cell disruption was confirmed by phase contrast microscopy. After removal of the glass beads and unbroken cells, the crude extract was centrifuged at 100,000 × *g* for 30 min at 4°C. The supernatant and the pellet, S100 and P100 fractions, were analyzed by immunoblot. For cell wall isolation, 50 OD_{450} units of cells were mechanically broken in 300 μl of SDS sample buffer supplemented with the protease inhibitors as described above. After removal of the glass beads and centrifugation of the crude extract for 1 min at 400 × *g*, the pellet contained the cell walls. The cell walls were processed essentially as described previously (de Groot *et al*., 2004). They were washed with 1 ml of 1 M NaCl at 4°C and boiled once at 100°C for 5 min in 1 ml of a buffer A (2% SDS, 40 mM β-mercaptoethanol, 100 mM EDTA, and Tris-HCl, pH 7.8), spun down, and then boiled again. After five washes with 1 ml of dH_2O the pellet was suspended either in 50 μl of 50 mM Tris-HCl, pH 7.4 containing 20 U of Quantazyme, a recombinant β(1,3)-glucanase (Qbiogene Europe, Illkirch, France) or in 50 μl of 50 mM MES, pH 6.0, containing 30 mU of laminarinase, a β(1,3)-glucanase preparation (Sigma-Aldrich), or in 70 μl of 50 mM MES, pH 6.0, supplemented with 30 μl of pure exochitinase of *Serratia marcescens* (~30 μg of the purified enzyme), kindly provided by Dr. Enrico Cabib (National Institutes of Health, Bethesda), and protease inhibitors. After a 16-h incubation at 37°C for Quantazyme and at 30°C for exochitinase or 2 h at 37°C for Laminarinase under gentle shaking, the samples were centrifuged at 11,000 × *g* for 5 min, and the supernatants were analyzed by immunoblot. In the sequential treatments, the pellet of the first digestion was boiled in buffer A for 10 min to inactivate the enzyme. After five washes with dH_2O, the pellet was digested in 70 μl of 50 mM MES, pH 6.0, supplemented with 30 μl of pure exochitinase and the exochitinase pellet in 50 μl of 50 mM Tris-HCl, pH 7.4, containing 20 U of Quantazyme or in 50 μl of 50 mM MES, pH 6.0, containing 30 mU of laminarinase. After 2 h (laminarinase) or overnight digestion (Quantazyme and exochitinase) at 37 or 30°C (exochitinase), the samples were centrifuged and the supernatants were denatured. When the exochitinase treatment of the glucanase-released fraction was performed, the supernatant from the glucanase digestion was supplemented with 30 μl of exochitinase and incubated overnight (30°C). After centrifugation, the supernatant was analyzed. The samples were denatured in SDS-sample buffer for SDS-PAGE and immunoblot. SDS-PAGE was performed using 7% polyacrylamide slab gels (14 × 16 cm).

DRM Isolation

Isolation of the DRMs was performed essentially as described previously (Bagnat *et al*., 2000). Yeast cells (25 OD_{450}) were mechanically broken in a FastPrep 120 in 500 μl of TNE buffer (50 mM Tris-HCl, pH 7.4, 150 mM NaCl, and 5 mM EDTA) supplemented with protease inhibitors and glass beads as described above. The lysates were cleared by centrifugation at 500 $\times$ *g* for 5 min at 4°C. Two cleared lysates were pooled and incubated with 1% Triton X-100 for 30 min at 4°C. The lysate (1.5 ml) was adjusted to 40% Opti-Prep (Sigma-Aldrich), and the resulting mixture (4.2 ml) was sequentially overlaid with 6.7 ml of 30% Opti-Prep in TNEX buffer (TNE buffer including 0.1% Triton X-100) supplemented with protease inhibitors and 1.1 ml of TNEX buffer. The samples were centrifuged at 100,000 $\times$ *g* in SW41Ti rotor for 2.5 h. At the end, 0.9-ml fractions were collected from the top of the gradient. Proteins were precipitated with 10% TCA on ice and analyzed by Western blot.

RESULTS

Construction of Fluorescent Versions of Gas1p

Gas1p is processed and transported to the plasma membrane through the secretory pathway (Popolo and Vai, 1999). Besides an N-terminal signal peptide required for targeting to the endoplasmic reticulum (ER), Gas1p has also a C-terminal signal sequence that directs the GPI attachment to the newly synthesized precursor. Because both these sequences are required for the maturation of Gas1p, we created internally tagged versions of *GAS1* gene. In the first construct an mRFP was fused, in-frame, to the *GAS1* coding sequence following the signal peptide (Figure 1A). This construct was previously described by others and used for a different purpose (Fujita *et al*., 2006). In the second construct, we inserted a bright version of GFP between the residues G486 and T487, within the Ser-rich region (Figure 1C). We chose this site on the basis of two criteria: 1) the Ser-rich region functions as a spacer and is dispensable for in vivo functionality and in vitro activity of Gas1p (Gatti *et al*., 1994, Carotti *et al*., 2004) and 2) the insertion site is downstream the two functional domains, GH72 and Cys-box, that are essential for Gas1p functionality (Popolo *et al*., 2008). The expression of both mRFP-Gas1p and Gas1p-GFP was driven by the natural *GAS1* promoter. The fusion genes were either integrated into the genome (mRFP-*GAS1*) or placed on episomic plasmids (*GAS1*-GFP).

To establish whether the fusion proteins were functional, we tested their capability to suppress the defective phenotype of *gas1*Δ cells (Popolo *et al*., 1997; Valdivieso *et al*., 2000). As shown in Figure 1, A and B, mRFP-Gas1p fully complemented the CF hypersensitivity of *gas1*Δ cells and also suppressed other phenotypic traits such as the round morphology, the larger cell size and defective bud maturation and cell separation, these last two traits being responsible for the appearance of "mickey mouse" cells and the clumpy phenotype of *gas1*Δ cells (Popolo *et al*., 1993b). Moreover the reduced growth rate (μ) of *gas1*Δ cells (0.24 $\pm$ 0.02 h^{-1}) reverted to the value of the parental strain (0.66 $\pm$ 0.05 h^{-1}), as the growth rate of the strain expressing mRFP-Gas1p was 0.65 $\pm$ 0.04 h^{-1}. Thus mRFP-Gas1p fully suppressed the defective *gas1*Δ phenotype.

Plasmids harboring the *GAS1*-GFP gene were introduced into a *gas1* diploid null mutant derived from AN120 (see Table 1). Transformed cells were propagated in selective SD plates but inoculated in YPD because Gas1p-GFP did not mature into the fully glycosylated form and was not fluorescent in cells growing in liquid SD (our unpublished data). In YPD, *GAS1*-GFP complemented the CF hypersensitivity of *gas1* cells when placed either on single or multicopy plasmids similarly to the plasmid carrying the wild type *GAS1* (Figure 1C). *GAS1*-GFP placed on single or multicopy plasmids partially suppressed the slow growth rate of *gas1*Δ.

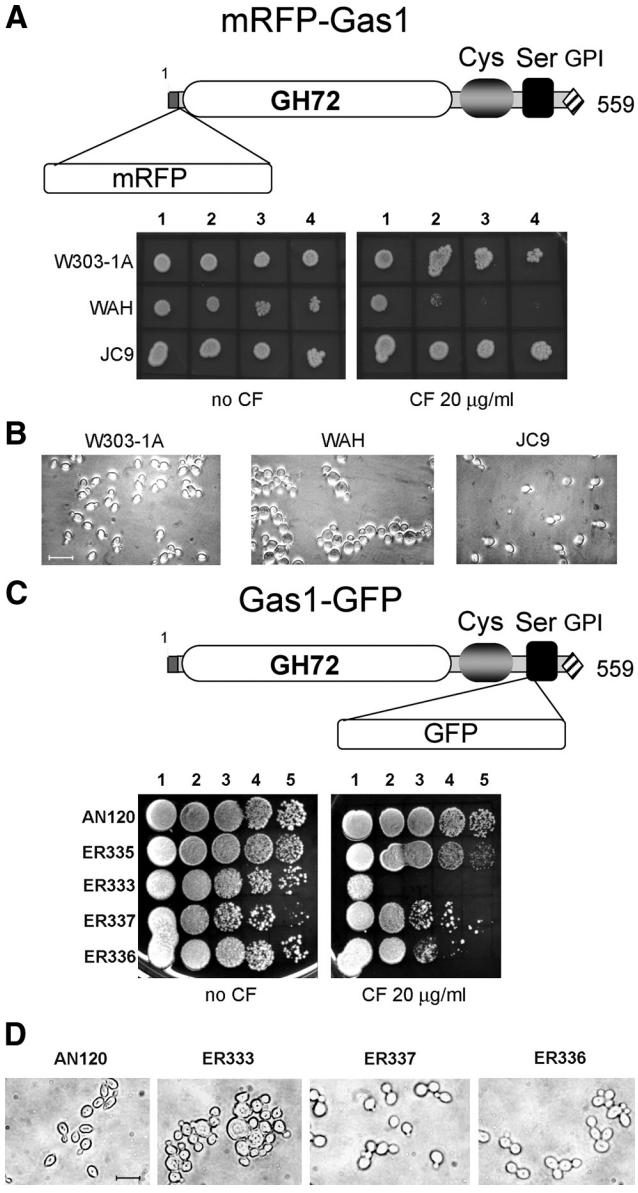

Figure 1. Fusion to fluorescent proteins results in a functional Gas1 protein. (A and C) Schematic diagrams of the domain organization and site of insertion of the fluorescent proteins. The gray box represents the signal peptide. GH72, signature domain of GH72 glycosylhydrolases; Cys, cysteine-enriched module; Ser, serine-rich region and GPI, signal for GPI attachment at N528. For the CF sensitivity assays, cells were grown to log phase in YPD at 30°C. Ten-fold dilutions, from 2 to 4, of the concentrated suspension 1 of W303-1A, a derived *gas1*Δ mutant (WAH) and JC9, a *gas1*Δ mutant harboring an integrated copy of mRFP-*GAS1*, were prepared and spotted on YPDA plates. After 48 h at 30°C the plates were photographed. The CF assay for the Gas1-GFP was performed as described in A by using cells grown in YPD at 30°C of the diploid AN120 strain, a derived homozygous *gas1*Δ mutant carrying YEp24-*GAS1* (ER335), YEp24 (ER333), YEp24-*GAS1*-GFP (ER337), or pRS416-*GAS1*-GFP (ER336). (B and D) Morphology of Formalin-fixed cells.

The growth rates were 0.46 $\pm$ 0.04 and 0.44 $\pm$ 0.04 h^{-1}, respectively, compared with a value of 0.32 $\pm$ 0.06 for the *gas1* null mutant transformed with the empty vector and 0.55 $\pm$ 0.02 h^{-1} for the parental AN120 strain. The clumpy phenotype, the round shape and the large size were greatly

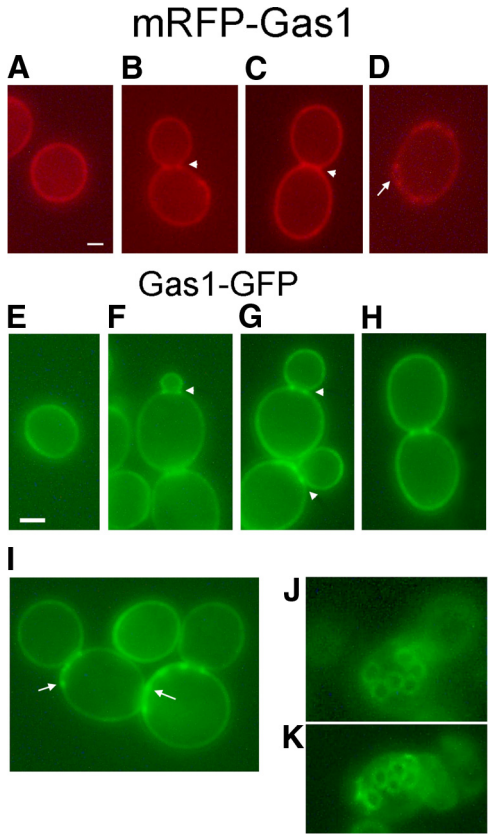

Figure 2. mRFP-Gas1 and Gas1p-GFP fluorescent proteins are associated to the plasma membrane, bud neck, septum and bud scars. (A–D) Cells of the haploid strain JC9, a *gas1*Δ expressing mRFP-Gas1p from a construct integrated into the genome, were grown in YPD at 30°C. Cells were fixed and washed with PBS, pH 7.4, before microscopy observation. Bar, 1 μm. (E–K) Cells of the diploid strain ER336 (a diploid *gas1*Δ mutant carrying the single copy plasmid pRS416-*GAS1*-GFP) were grown to log phase in YPD at 30°C. Cells were observed in PBS without fixation. Arrowheads, two dots aside the neck or septum. Arrows, bud scars. Bar, 3 μm.

attenuated in strains expressing Gas1p-GFP (Figure 1D). The construct restored the ellipsoidal morphology more completely when placed on a single copy plasmid as shown by the presence of more elongated cells in strain ER336. In contrast, the defect of cell separation was better complemented by the multicopy plasmid.

Gas1p Is Localized at the Cell Periphery, at the Mother-Daughter Neck Region, in the Septum and in Bud Scars

mRFP-Gas1p expressed in a *gas1*Δ mutant exhibited various locations. It decorated the cell periphery consistently, illustrating the plasma membrane localization of the protein (Figure 2). In addition, in medium-budded cells the fluorescence appeared as two bright dots at either side of the mother-daughter neck region and in large-budded cells clearly decorated the entire septum region (Figure 2, B and C). Interestingly, fluorescent rings or crater-like structures were observed, suggesting that mRFP-Gas1p was also localized in the bud scars (Figure 2D). In addition, we also detected bright crescent-shaped fluorescent segments at the edge of cells. These may represent lateral views of one or more adjacent bud scars (Figure 2D). When mRFP-Gas1p was expressed in the parental strain it was detected in perinuclear structures, in addition to the localization pattern previously described, suggesting a partial retention in the ER, probably due to competition in folding with endogenous Gas1p (data not shown).

Next, we analyzed the localization of Gas1p-GFP in a *gas1*Δ mutant. Gas1p-GFP localized to the plasma membrane (Figure 2E), in the mother-daughter neck (Figure 2, F–H), in the septum of large-budded cells (Figure 2H) and in bud scars (Figure 2, I–K). Similar results were also obtained for the Gas1p-GFP fusion expressed in the parental strain indicating that, for this hybrid protein, no competition with the endogenous protein occurs. The same pattern of localization was observed when the hybrid *GAS1-GFP* gene was placed either on single copy or multicopy plasmids. These data show that Gas1p maintains the same localization regardless of the type of fluorescent protein, site of fusion, genetic background or ploidy and gene dosage of the construct.

For a complete view of the various regions where Gas1p localizes, a stack acquisition was performed. Figure 3 shows surface and transversal sections of representative cells. In a small-budded cell, Gas1p-GFP is distributed in the cell periphery with a preferential location around the bud (Figure 3A). A bright fluorescent ring was visible in the surface sections supporting the inference that Gas1p-GFP was localized in a bud scar (Figure 3A, 1–3). In cross sections around the medial plane, the bright fluorescent structure present at the mother-daughter neck was visibly a ring (Figure 3A, 5–7). In the cross sections 6–8, a crater-like structure close to the neck was clearly visible. In the surface planes 1 and 2 and 8 and 9 of Figure 3A, a punctate pattern of very fine patches or dots was visible. Figure 3B shows a large-budded cell with a bright fluorescence in the septum area (Figure 3B, 2–4). In the medial plane Gas1p-GFP filled the inner part of the septum suggesting that the protein colocalizes with the chitin disk present at the primary septum (Figure 3B, 3 and 4). In surface sections the fluorescence was distributed in very fine dots all over the cell (image *1*) and in discrete sites on the cell contour (images 1 and 2 and 7 and 8).

Figure 3C shows two magnifications of representative images of surface sections. A punctate pattern of fine fluorescent dots is clearly visible. This pattern is consistent with the localization of the plasma membrane Gas1p-GFP in lipid rafts as indicated in previous biochemical reports (see Introduction). In Figure 3C, a fluorescent ring of Gas1p-GFP is also clearly visible. The brightness of the ring suggests that Gas1p is concentrated in these structures. In conclusion, these analyses demonstrate that Gas1p localizes in three districts: at discrete sites of the plasma membrane, in a ring at the mother-daughter neck and in the bud scars. In addition, these experiments suggest a fourth unexpected localization of Gas1p, in the primary septum.

To determine whether Gas1p-GFP associates with the lipid rafts, we used a biochemical approach to isolate the DRMs. A hallmark behavior of DRMs is their low-buoyant density after detergent extraction and centrifugation in iodixanol (e.g., Opti-Prep) discontinuous step gradients (Bagnat *et al.*, 2000). Gas1p-GFP was recovered in fraction 2 at the top of an Opti-Prep gradient showing the same behavior of wild type Gas1p (Figure 3, D and E). The apparent molecular mass of Gas1p-GFP was ~155 kDa in accordance with the size expected for a polypeptide constituted by Gas1p (~125 kDa) and GFP (~30 kDa). Another form of Gas1p-GFP (~120–130 kDa) was abundant in fractions 7–9 of the gradient, suggesting an intracellular accumulation of immature forms (Figure 3D). These results extend the microscopy

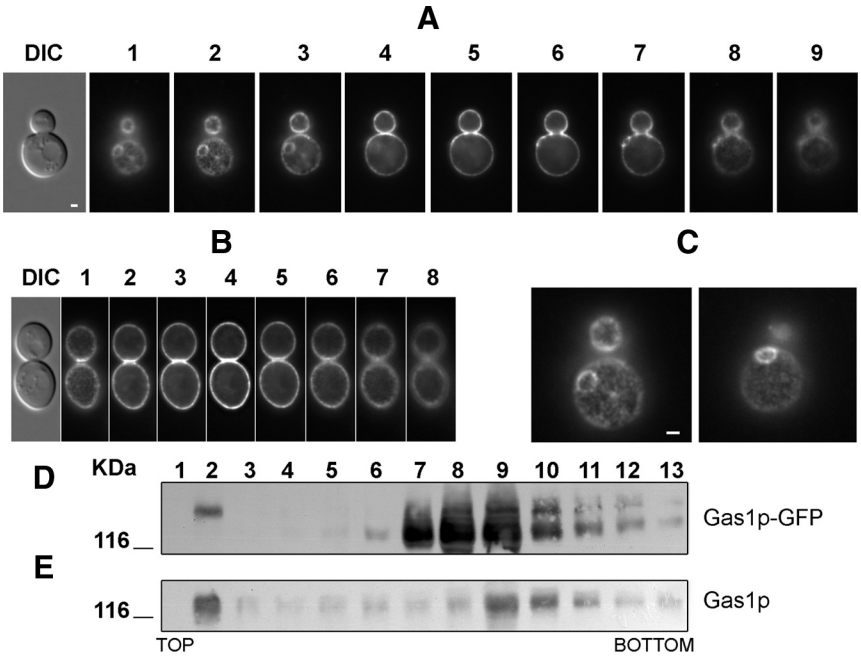

Figure 3. Gas1-GFP protein has multiple locations in the single cell. Cells of strain ER337, a *gas1*Δ homozygous diploid mutant carrying the plasmid YEp24-*GAS1*-GFP were photographed through a fluorescence microscope equipped for stack acquisition. Optical sections of 400-nm intervals through individual cells are shown. (A) Small-budded cell, images 1–3: surface sections showing a ring and pattern of small dots all over the membrane. Images 4–7, in cross sections, the fluorescence forms a ring at the mother-daughter neck. Images 6–8, sections showing a bud scar next to the bud neck. (B) Large-budded cell, images 1 and 2 show the small dots pattern over the plasma membrane. Images 3–5, the fluorescence is inside the septum region. Images 6–8, surface sections showing a punctuate pattern in the membrane. (C) Magnification of surface sections of small-budded cells with a visible bud scar. Bar, 1 μm. (D and E) Gas1-GFP associates with the detergent-resistant membranes. Cell extracts were treated as described under *Materials and Methods*. Fractions (1–13) of the density gradient were collected from the top. (D) Immunoblot of fractions from ER366 strain, a *gas1*Δ mutant harboring pRS416-*GAS1*-GFP, obtained using anti-GFP monoclonal antibody. (E) Immunoblot from AN120 parental strain obtained using anti-Gas1p polyclonal serum.

analysis and provide further support for the localization of Gas1p-GFP in the lipid rafts.

mRFP-Gas1p Is in Mobile or Immobile Pools Depending on Its Localization

In experiments originally designed to study Gas1p localization in conditions of α-F–induced polarized growth, we noticed that the mRFP-Gas1p fluorescence around the cell rapidly decreased after addition of α-F to the culture. In these studies *MATa gas1*Δ cells expressing mRFP-Gas1p were treated with α-F, and the effect on cell cycle progression was monitored by measuring the decrease of budding index and the appearance of shmoos (Figure 4A). 3.25 h after the addition of α-F, the red fluorescence signal at the cell contour was greatly reduced except at the bud scars and in the rare septa that were still fluorescent (Figure 4B). This suggested that mRFP-Gas1p in the membrane could be labile, whereas the association to the bud scar could protect it from degradation.

To further analyze this hypothesis, we determined the levels of the Gas1 and fusion proteins in total lysates at different time intervals after addition of α-F. As shown in the immunoblot of Figure 4C, Gas1p migrated as an ~125-kDa polypeptide and mRFP-Gas1p as an ~155-kDa band. After addition of α-F, the intensity of the 125-kDa band did not significantly change, whereas the 155-kDa band seemed to rapidly diminish being undetectable after 3.25 h of treatment. The level of Gas1 and mRFP-Gas1 polypeptides was normalized for the intensity of the actin band. As shown in Figure 4D, Gas1p remained approximately constant whereas mRFP-Gas1p levels decreased markedly during the treatment with α-F. Moreover, at time zero the steady-state level of mRFP-Gas1p was ~50% the level of Gas1p, suggesting that mRFP-Gas1p is either less synthesized or degraded more rapidly than Gas1p in vegetative growth. Because *GAS1* expression is turned off and its mRNA levels rapidly decrease during α-F treatment (Popolo *et al*., 1993a), these experiments point to an increased rate of degradation of mRFP-Gas1p compared with Gas1p. Therefore the reduction of mRFP-Gas1p in the cell contour observed in the microscopy analysis is more likely to be due to the removal of the protein from the plasma membrane caused by high turnover and to the absence of de novo synthesis.

We studied the localization of the fluorescent labeling that persisted during α-F treatment in more detail. We performed confocal microscopy analysis using Calcofluor to stain chitin (blue fluorescence) in cells expressing mRFP-Gas1p. During vegetative growth, mRFP-Gas1p was visible all over the cell with an increased concentration in the bud scars (Figure 5A). In cells treated for 3.25 h with α-F, the red fluorescence around the cell decreased but the signal colocalized with chitin in the bud scars remained intense (Figure 5A, bottom). These results indicate that mRFP-Gas1p undergoes a high turnover in the plasma membrane, whereas it is stabilized when localized to the bud scar. This particular behavior was specific to this fusion at the N-terminal end of Gas1p. We took advantage of it as a tool to further investigate the localization to the bud scar.

The Immobile Form of Gas1p Is Cross-Linked to the Cell Wall

We reasoned that if a fraction of mRFP-Gas1p was associated with the plasma membrane and another was covalently bound to the cell wall, in α-F–treated cells we should still detect mRFP-Gas1p bound to the cell wall fraction but not the fraction present in the plasma membrane. At time 0 and 3.25 h after α-F addition, different subcellular fractions and purified cell walls were obtained according to the scheme shown in Figure 5B. As shown in the immunoblot of Figure 5C, in untreated cells both Gas1p and mRFP-Gas1p were detected in the membrane fraction. After treatment with α-F, Gas1p was enriched in the membrane fraction whereas mRFP-Gas1 was not detectable in either the total or membrane fractions.

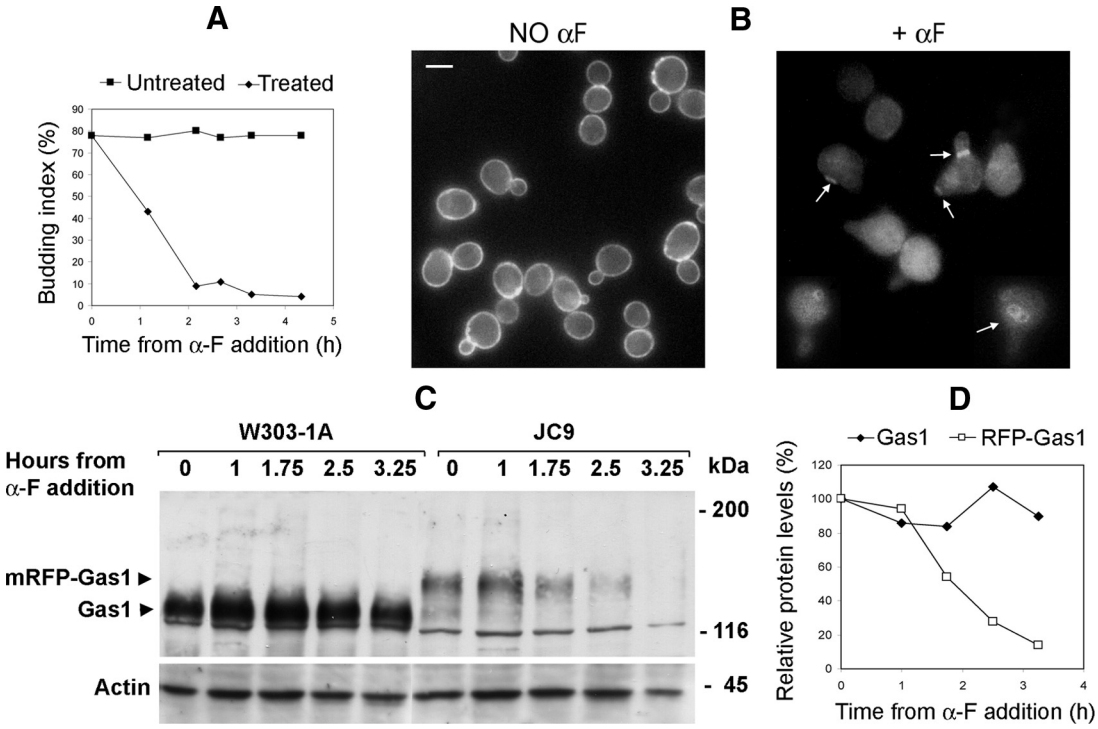

Figure 4. mRFP-Gas1p is produced as an unstable 155-kDa polypeptide that is rapidly removed from cell contour in α-F–treated cells. (A) Cells from an exponentially growing culture were treated with 20 μg/ml α-F. A representative plot of the percentage of budded cells in W303-1A or JC9 strain is shown. (B) Microscopy analysis of mRFP-Gas1p. Cells were collected, fixed, and then washed with PBS. The fluorescence is present at the cell periphery, in the neck and bud scars as previously shown in Figure 2, but after 3.25 h of α-F only bud scars or septa are bright (arrows). Bud scars are on a focus plane that makes the cell fluorescence diffuse. Bar, 3 μm. (C) Immunoblot of total protein extracts (~80 μg) from W303-1A and JC9 cells at different time from α-F addition. (D) Relative protein levels of Gas1p and mRFP-Gas1p determined by densitometric analysis of the bands of the immunoblot shown in C. Similar results were obtained in two independent experiments.

To determine whether Gas1 and mRFP-Gas1 proteins remain bound to the cell wall, we treated purified cell walls with a β(1,3)-glucanase preparation (laminarinase) or with pure exochitinase (fractions G and Exo, respectively, in Figure 5B). Before α-F addition, Gas1p and mRFPGas1p were readily released by both treatments (Figure 5D, lanes 1 and 2, G and Exo panels). This indicates that a pool of Gas1p is linked to β(1,3)-glucan and another to chitin. Similar results were obtained using Quantazyme, a recombinant β(1,3)-glucanase (data not shown). After treatment with α-F, both Gas1p and mRFP-Gas1p were still present in the β(1,3)-glucanase-released material, indicating that this pool is stably anchored to the cell wall (Figure 5D, lanes 3 and 4, G panel). Unexpectedly, neither protein was released by exochitinase (Figure 5D, lanes 3 and 4, Exo panel). We hypothesized that the pool bound to chitin could possibly be converted into an insoluble exochitinase-resistant form and new synthesis of the chitin-bound pool did not occur during α-F arrest. Because a CWP can be simultaneously linked to chitin and β(1,3)-glucan (Kollar *et al*., 1997), we treated the glucanase-resistant fraction with exochitinase and vice versa (fractions G-Exo and Exo-G in Figure 5B). The increased amount of Gas1p recovered in the G-Exo fraction (Figure 5D, lanes 3 and 4) supports the hypothesis that Gas1p linked to chitin could be further anchored to glucan in α-F–treated cells. However, because insoluble material still remained after the sequential digestions we cannot exclude that the chitin-bound Gas1p form, presumably present in the bud scars, could be resistant to the enzymatic extractions used.

These experiments indicate the existence of a new form of Gas1p linked to chitin. The complex is detected in proliferating cells but not in cell arrested in G1 by α-F treatment. Another fraction of Gas1p is linked to β(1,3)-glucan and extractable by β(1,3)-glucanase as reported previously (De Sampaio *et al*., 1999). This fraction is probably distributed all over the cell wall and corresponds to the faint signal detected by fluorescence microscopy after α-F arrest. Results supporting this hypothesis will be further described and discussed below (see Figure 9 and Discussion).

Chs3p-dependent Chitin Synthesis Mediates Gas1p-GFP Localization into the Chitin Ring

To study whether the anchoring of Gas1p to the chitin ring and bud scars requires chitin synthesis mediated by Chs3p—the enzyme responsible for the formation of the chitin ring—we examined the localization of Gas1p in a strain deleted for *CHS3*. As expected in *chs3*Δ cells, chitin ring and bud scars were absent, budding was abnormal, elongated bud necks were often observed and gave rise to protuberances after cell separation as previously described for *chs3* null mutants (Shaw *et al*., 1991). In the *chs3*Δ mutant Gas1p-GFP was absent at both sides of the mother-daughter neck but was present all over the plasma membrane (Figure 6A, top). In addition, Gas1p-GFP was detected as a thin line inside the septum of binucleate cells where chitin synthesized by Chs2p forms the primary septum (Figure 6A, bottom). About one-third of the cells had an elongated neck region and the septum was curved as previously observed

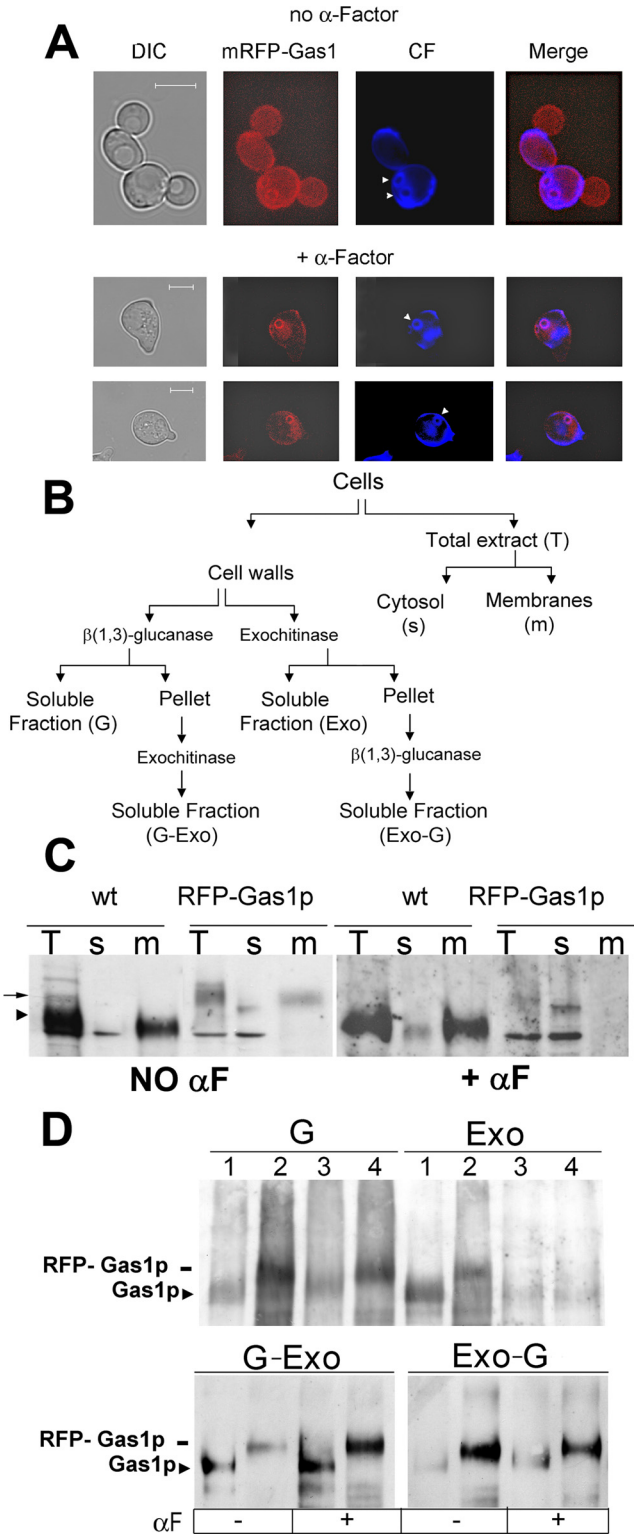

Figure 5. mRFP-Gas1p colocalizes with chitin in the bud scars. (A) JC9 cells, carrying an integrated mRFP-*GAS1* copy, were grown to log phase in YPD at 30°C and treated for 3.25 h with α-F. Cells were collected and analyzed without fixation with a confocal microscope. The images are the result of superimposed optical sections. Cells show CF staining of chitin (blue fluorescence) and mRFP-Gas1p (red fluorescence). In vegetative growth, mRFP-Gas1p was distributed at the cell periphery and also clearly colocalized with the bud scars as detected by the merging of the red and blue fluorescence, which produced a light pink color. In cells treated with α-F the red fluorescence in the periphery decreased but it was still very intense in the bud scars colocalizing with the chitin signal. Bar, 5 μm. (B) Flow chart of subcellular fractionation and cell wall treatments. (C) Immunoblot analysis with anti-Gas1p polyclonal antibodies of total protein extracts, soluble and membrane fractions from W303-1A and JC9 cells before (left) and after 3.25 of α-F treatment (right). Arrowhead: Gas1p; arrow: mRFP-Gas1p. A sharp band of about 100 kDa is a cross-reactive polypeptide. (D) Immunoblot of the cell wall fractions obtained and designated according to the scheme in C. Lanes 1 and 3, W303-1A cells; lanes 2 and 4, JC9 cells.

for *chs3*Δ mutants (Figure 6B; Shaw *et al*., 1991). In these cells, the line of the green fluorescence was also curved (Figure 6B). The same results were obtained when GAS1-GFP was on single or multicopy plasmids.

To further refine the localization in the septum, Gas1p-GFP and chitin (blue fluorescence) were examined with the confocal microscope. In the wild-type cells, the septum was thick and very bright and the green and blue fluorescence overlapped (Figure 6C). The strong green signal resulted from the sum of the fluorescence of the primary septum and chitin ring. In the *chs3* null mutant the septum seemed to be less bright with a uniform thickness and did not reach the cell contour in agreement with the lack of the chitin ring (Figure 6D). A merge of optical section series of the septum indicated that both chitin and Gas1p-GFP fluorescence form a disk in the septum (not shown in Figure 6). These results indicate that Gas1p is localized in the primary septum or in close proximity to it.

Localization of Gas1p-GFP in the chs2Δ and chs1Δ Mutants

To further explore the interaction of Gas1p with the chitin of the primary septum we determined the localization of Gas1p in a *chs2*Δ mutant. The lack of Chs2p is known to be compensated by the synthesis of a thick "remedial" septum that is amorphous and devoid of the trilaminar structure typical of a normal septum (Shaw *et al*., 1991). This septum is rich in chitin produced by Chs3p, which becomes essential for the survival of *chs2*Δ cells (Cabib and Schmidt, 2003). Remedial septa also contain cell wall material deposited in an orientation parallel to the mother-bud axis instead of perpendicular as occurs when the primary septum is present. As shown in Figure 7A, Gas1p-GFP exhibited a heterogeneous localization in a *chs2*Δ mutant strain. In cells which displayed an elongated septum, the fluorescence of Gas1p-GFP was faint, diffuse and distributed over the length of the septum. Gas1p-GFP was more abundant in thicker septa. Filaments with frayed ends were also detected as protruding from the bud scar (Figure 7A). This indicates that Gas1p-GFP accumulates in the remedial septa in aberrant arrangements probably as part of the cell wall material. Altogether, these observations led us to conclude that Gas1p-GFP localization in the septum is markedly disturbed in *chs2*Δ mutant cells. The effect could be due both to the absence of the deposition of chitin in the primary septum and to the synthesis of the remedial septum.

To further examine the interaction with chitin synthases, we analyzed the localization of Gas1p in a *chs1*Δ mutant but we could not detect any notable change in the major localization sites of Gas1p-GFP (Supplemental Figure S1).

Gas1p Is Released into the Medium in chs1Δ, chs2Δ, and chs3Δ Mutants

Our results suggest that Gas1p-GFP localization in the bud neck, bud scars, and septum is dependent on deposition of

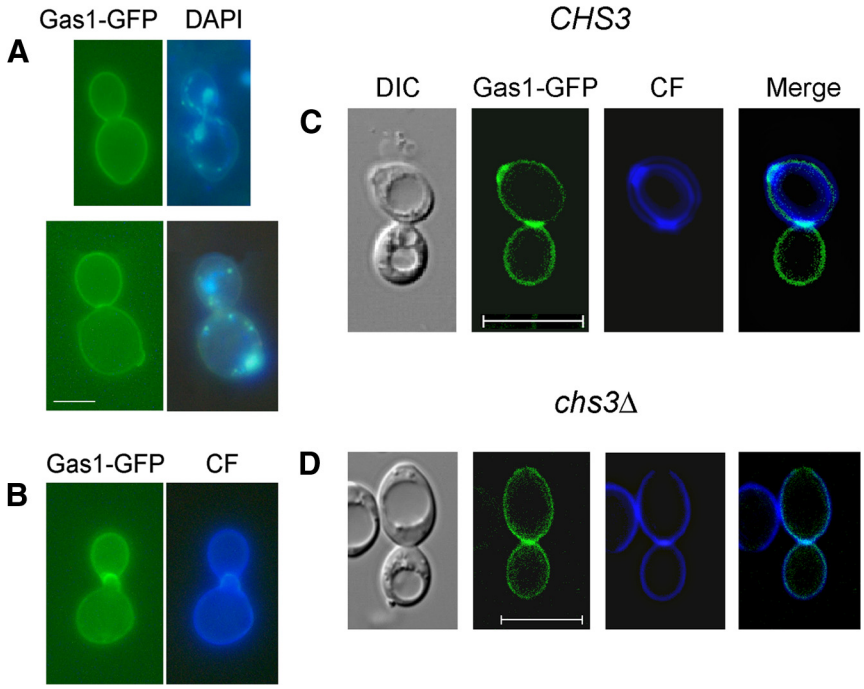

Figure 6. Localization of Gas1p-GFP in *chs3*Δ mutant cells. (A) Top, a diploid cell of strain ER344 (*chs3*Δ) undergoing mitosis lacks Gas1p-GFP in the mother-daughter neck region. Bottom, a representative cell at citokinesis with Gas1p-GFP along the septum line. (B) Haploid cell of strain *chs3*Δ-*GAS1-GFP* shows a curved septum and an elongated neck. Gas1p-GFP is present at the septum. CF, calcofluor staining of chitin. Bar, 2.5 μm. (C and D) Confocal microscopy of wild-type and *chs3*Δ cells expressing Gas1p-GFP. The images are the result of superimposed optical sections. The merge of the green and blue fluorescence generates a light blue. (C) The wild-type diploid cell (strain ER342) shows a bud scar and a septum region. (D) A *chs3*Δ cell (strain ER344) shows a less brilliant septum region consistent with the lack of the chitin ring and Gas1p-GFP localization at the primary septum. The superimposition of CF fluorescence produced a double fluorescence at the cell contour which is due to the roundness of the cell. Bar, 10 μm.

chitin. We reasoned that mutants deleted in genes encoding chitin synthases could release Gas1p into the growth medium. We monitored the presence of wild-type Gas1p in cell lysate and medium fraction from cell cultures of *chs1*Δ, *chs2*Δ, *chs3*Δ mutants and their isogenic strain. The results are shown in Figure 7B. Gas1p was present at similar levels in the cell lysates from the four strains. Interestingly, Gas1p was detected in the culture medium of *chs1*Δ, *chs2*Δ, and *chs3*Δ cells, whereas no appreciable amount of Gas1p was recovered from the parental strain. This indicates that the cross-linking of Gas1p to the cell wall depends on chitin synthesized by Chs2p (primary septum) or Chs3p (bud neck and scar) in accordance with the results shown in Figures 6 and 7A. Moreover the medium from the *chs2*Δ culture seemed to contain a higher amount of Gas1p compared with the other mutants.

Surprisingly, we also found Gas1p in the medium of a *chs1*Δ culture. It has been reported that *chs1*Δ daughter cells undergo lysis when the external pH becomes highly acidic, a condition that hyperactivates chitinase (Cabib *et al.*, 1989). Therefore, we grew the cells both in YPD, where the pH drops during growth, and in YPD buffered at pH 6.5. At pH 6.5, Gas1p was still released into the medium although at a lower level with respect to cells grown in unbuffered YPD (Figure 7C). Thus, we can conclude that chitin synthases or their products are required for the binding of Gas1p to the chitin ring (bud scar), septum and also to repair chitin.

Conversion of Gas1p into a Transmembrane Protein Prevents Localization of Gas1p to the Chitin Ring, Bud Scars, and Primary Septum and Affects Cell Separation

To determine whether cross-linking at the chitin ring and septum depends on GPI, we replaced the portion encoding the C-terminal region of Gas1p with the transmembrane (TM) domain and cytosolic tail of Mid2p (see scheme in Figure 8A). The C-terminal portion of Gas1p included the Ser-rich region and the GPI-attachment signal. In this way, Gas1p was converted into a type I TM protein. Mid2p has a uniform distribution in the plasma membrane and acts as a sensor of cell wall stress, but it is not functional when devoid of the extracellular portion (Straede and Heinisch, 2007). The chimera mRFP-Gas1-Mid2p was detected as an ~140-kDa polypeptide (data not shown). The growth rate (μ; h^{-1}) of the W303-1A, *gas1*Δ strains and the *gas1*Δ strain expressing the mRFP-Gas1p or the mRFP-Gas1-Mid2 protein were 0.66, 0.24, 0.66, and 0.55, respectively, indicating that the chimera suppressed the slow-growth rate defect of the mutant although not as efficiently as mRFP-Gas1p. In cells expressing the chimera, we noticed an incomplete suppression of the morphological defects of *gas1*Δ cells. Approximately 15% of the cells remained attached in two, three or four cells groups, a phenotype not observed for cells expressing the mRFP-Gas1 full-length protein.

The hybrid protein was localized at the cell periphery demonstrating that it is transported to the cell surface (Figure 8B). In some cells, an accumulation of the hybrid Gas1p close to the bud neck was also visible but we have not been able to detect any localization in the bud scar indicating that the apparent accumulation could be due to the curvature of the plasma membrane (Figure 8B, left). Interestingly, in groups of two or more unseparated cells, the red fluorescence labeled the cell contour but a thin gap was present in the middle of the septum region (Figure 8B, right). To further confirm these observations we performed confocal microscopy analyses that clearly showed the presence of the protein in the plasma membrane and its absence at the chitin ring of undivided cells (Figure 8C). Because the localization of Gas1p at the chitin ring was missing we could also confirm the lack of Gas1p in the primary septum underneath. These results reveal that cross-linking of Gas1p to the entire septum region relies on the presence of GPI.

We further monitored the effects of mRFP-Gas1-Mid2p on cell separation. We measured the fraction of cells with a genomic DNA content of 1, between 1 and 2, 2, and more than 2 by flow cytometric analysis Cells that are not completely separated are counted as a single unit in this analysis.

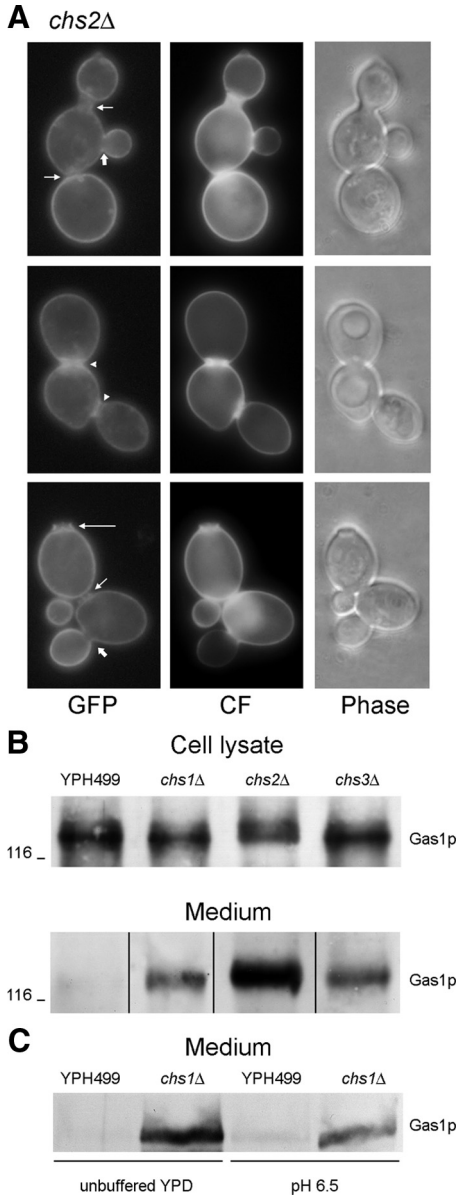

Figure 7. Localization of Gas1p is perturbed in a *chs2* null mutant. (A) CER5 (a *chs2*Δ mutant transformed with YEp24-*GAS1*-GFP) was analyzed during growth in YPD at 30°C. Short arrows indicate remedial septa with little Gas1p-GFP, arrowheads indicate thick remedial septa with bright Gas1p-GFP, the long arrow indicates an abnormal bud scar with filaments protruding and the thick arrows indicate necks with no Gas1p. (B and C) Cell lysates and proteins precipitated from the culture supernatants of the indicated strains, grown in YPD or in YPD buffered at pH 6.5, were analyzed by immunoblot with anti-Gas1p antibodies.

The profiles of the DNA content per cell are shown in Figure 8D. The percentage of cells with a DNA content >2C was ~5.5 in cells expressing mRFP-Gas1p and increased to 32.4 in the *gas1* mutant, whereas it was ~13 in cells expressing mRFP-Gas1-Mid2p. Thus, the TM form of Gas1p only partially relieves the cell separation defect of *gas1*Δ cells. In conclusion, both Gas1p forms, the one cross-linked to the septum region and the plasma-membrane GPI-anchored form, concur in facilitating cell separation.

We further characterized the effect of the chimera on the ability to suppress the phenotypic defects of *gas1*Δ cells. As shown in Figure 8E, the protein suppressed the CF hypersensitivity of *gas1*Δ cells, indicating that the hybrid protein was functional.

Loss of GAS1 Affects the Width of the Neck Region

To explore the role of Gas1p localization in the chitin ring, we investigated whether the lack of Gas1p could affect the size of the neck region. The neck region is a crucial constriction between the mother and daughter cells. It has been shown that the width of the neck region normally remains constant throughout the cell cycle (Cabib, 2004). The diameters of the mother-daughter neck, expressed as mean (μm) ± SD, in the parental strain W303-1A, *gas1*Δ cells and strain JC10, expressing mRFP-Gas1-Mid2p, were ~0.96 ± 0.16 (n = 15), 1.67 ± 0.29 (n = 20), and 1.45 ± 0.19 (n = 20), respectively. The enlargement of the bud neck suggests that the loss of Gas1p affects the rigidity of this region and that the cell wall-bound Gas1p contributes to this property.

Crh1 and Crh2 Transglycosylases Are Required for Immobilizing Gas1p into the Chitin Ring and Bud Scars

Crh1 and Crh2 enzymes have been proposed to assist the immobilization of specific GPI-CWPs to the bud scar through the binding of β(1,6)glucan to chitin (Cabib *et al*., 2008). Therefore, we analyzed the localization of Gas1p-GFP in the *CRH1*, *CRH2* single and double null mutants. The isogenic strain showed the normal localization of Gas1p (Figure 9A, top). In the single *crh1*Δ and *crh2*Δ mutants the localization of Gas1p was similar to the wild type with the exception that the fluorescent signal in the bud scars was weaker in the *crh2* single mutant (data not shown). Interestingly, in the double null mutant the fluorescence around the cell was intense whereas the green signal at the bud neck and bud scars was missing (Figure 9A, bottom). CF staining confirmed the presence of normal bud scars. This result indicates that Crh1 and Crh2 proteins are required for the immobilization of Gas1p-GFP to the chitin in the neck region and in the bud scars.

We also analyzed total lysates and cell wall fractions from exponentially growing cells. In a total lysate of the *crh1*Δ *crh2*Δ mutant, Gas1p was present at a level equivalent to the level of the parental strain (Figure 9B). The purified cell walls were treated with β(1,3)-glucanase (laminarinase) or pure exochitinase. The results are shown in Figure 9C. Gas1p was present in the glucanase-extractable material both in the parental strain and *crh1*Δ *crh2*Δ mutant indicating that the fraction of Gas1p readily extractable by β(1,3)-glucanase is not affected by the double deletion and, on the contrary, it seemed slightly increased (Figure 9C, lanes 1 and 2). Interestingly, Gas1p was released by exochitinase from the cells walls of the parental strain but not from the double mutant (Figure 9C, lanes 3 and 4). This experiment indicates that a putative GPI-Gas1p-β(1,6)-glucan-chitin complex is not produced in the absence of the Crh1and Crh2 proteins in agreement with the role of these enzymes in transferring chitin onto β(1,6)-glucan.

We hypothesized that the GPI-Gas1p-β(1,6)-glucan-chitin complex should not be extracted by exochitinase from *chs3*Δ cell walls. The digestion with exochitinase released Gas1p from the cell walls of the parental strain but not from the mutant (Figure 9C, lanes 5 and 6). Thus, both the lack of the cross-linking Crh enzymes or of the donor molecule abolishes the formation of the complex. As the Gas1p form released by exochitinase has an electrophoretic mobility very similar to that of the GPI-anchored Gas1p, the β(1,6)-glucan chain attached to Gas1p is likely to be very short.

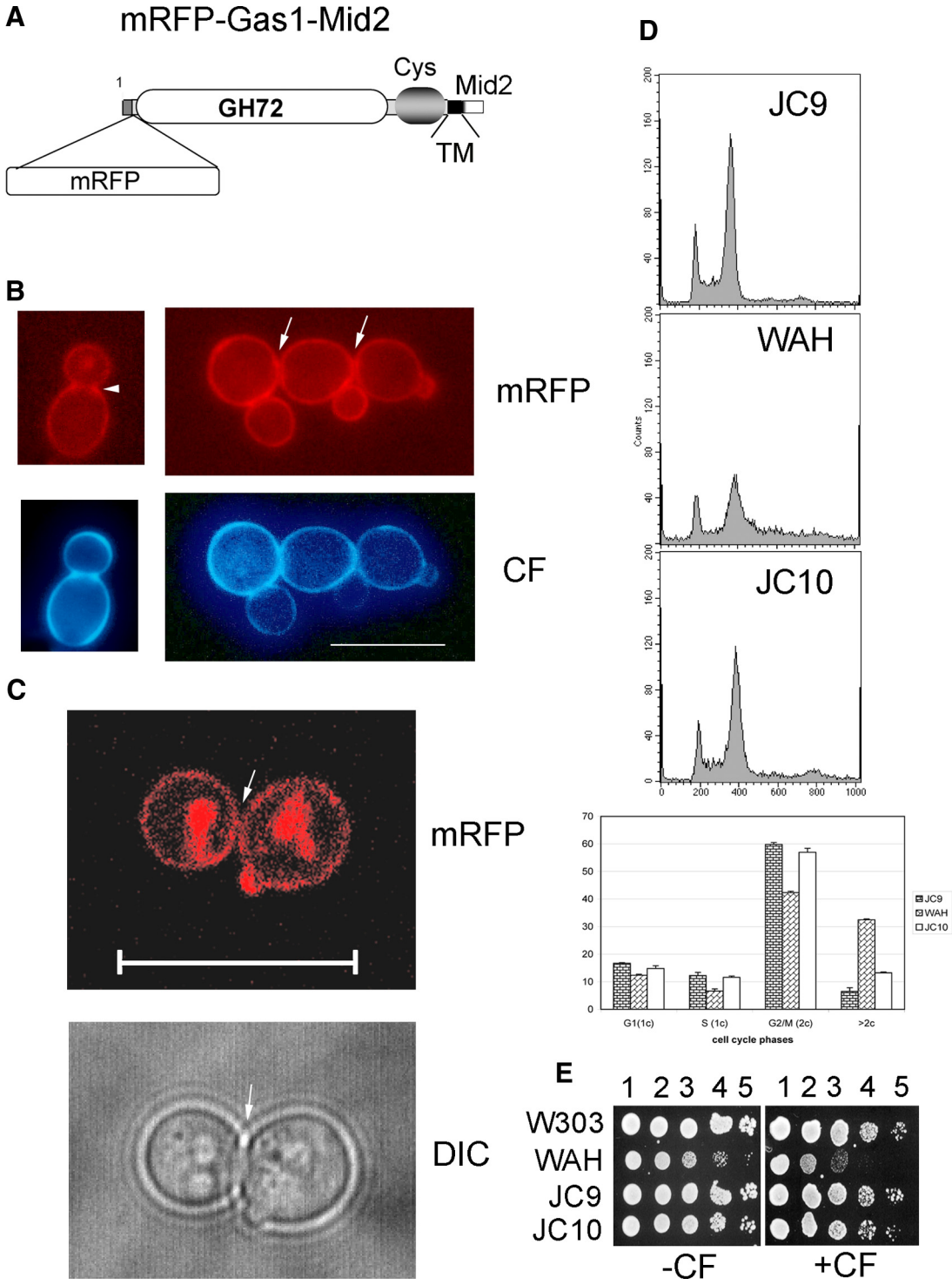

Figure 8. Conversion to a TM-form excludes Gas1p from the septum region. (A) Scheme of the fusion of the mRFPGas1-Mid2. (B) Representative JC10 cell (left) showing mRFP-Gas1-Mid2p in the plasma membrane (arrowhead) and chitin (blue) in the chitin ring. A group of three unseparated cells (right) shows the gap between membranes (arrows). Bar, 5 μm. (C) Confocal microscopy analysis shows in more detail the dark thin line which divides the two cells. The intracellular red fluorescence is due to partial retention of the hybrid protein in the ER. Bar, 10 μm. (D) Flow cytometric analysis of the DNA content per cell of the indicated strains. In the histogram the percentage of cells in the various compartments is shown. (E) CF sensitivity assay of the indicated strains.

As shown in Figure 9C (lanes 1 and 2), the electrophoretic mobility of the β(1,3)-glucanase-released form of Gas1p from BY4741 strain was heterogeneous (from 130 to >150 kDa). This could be consistent with the protein being covalently linked to β(1,3)-glucans with different accessibility to the enzymatic cleavage, to protein mannosylation or also with the presence of soluble chitin chains of different size. The digestion of the β(1,3)-glucanase-extractable material by

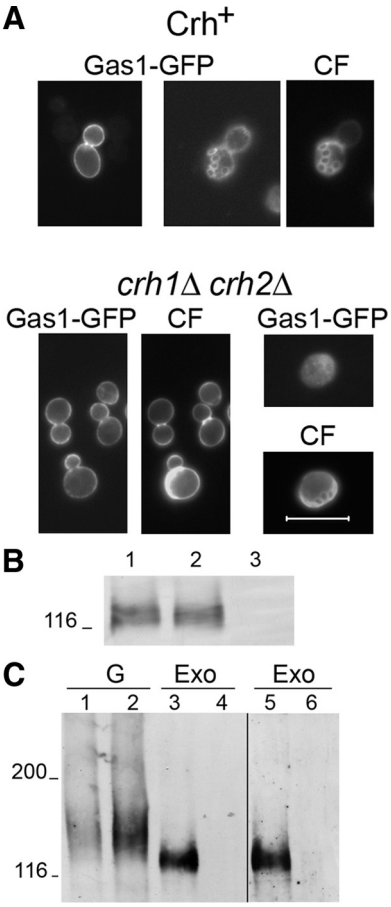

Figure 9. Crh1 and Crh2 enzymes are required for the cross-linking of Gas1p at the chitin ring and bud scar. (A) Fluorescence microscopy of Gas1p-GFP in the strains ER374 (Crh^+) and ER376 (*crh1*Δ *crh*Δ*2*). Gas1p-GFP is not present at the bud neck and bud scars. CF, calcofluor white staining of chitin. (B) Immunoblot of cell lysates with anti-Gas1p antibodies. Lane 1, BY4741; lane 2, *crhl*Δ *crh2*Δ (GRA007 strain); lane 3, *crh1*Δ *crh2*Δ *gas1*Δ. (C) Imunoblot of cell wall extracts with anti-Gaslp antibodies, G (laminarinase-extractable proteins) and Exo (exochitinase-extractable proteins). Lanes 1 and 3, BY4741; lanes 2 and 4, *crh1*Δ *crh2*Δ; lane 5, YPH499 and lane 6, *chs3*Δ mutant (ECY46-4-1B).

exochitinase did not affect the electrophoretic mobility of Gas1p suggesting that soluble chitin chains are not linked to Gas1p unless they are very short (data not shown).

DISCUSSION

Localization of Fluorescent Versions of Gas1p in Yeast Cells

The results reported in this work indicate that Gas1p has four distinct localizations in vegetative growing cells: it is present at the cell periphery, in the chitin ring, at the primary septum and in the bud scars where it remains for several generations (Figure 10). At the plasma membrane, we could visualize Gas1p-GFP in microdomains and then confirm biochemically that the fusion protein is recovered in the lipid rafts fraction. This result is consistent with early biochemical studies that reported the presence of Gas1p in plasma membrane derived DRMs (Bagnat *et al*., 2000). The localization of Gas1p here described also provides a possible explanation of the static behavior of a truncated derivative

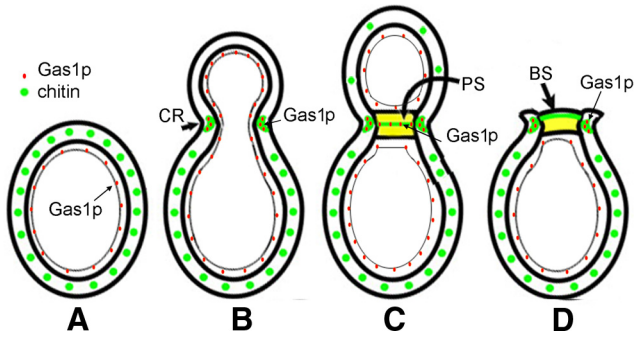

Figure 10. Scheme summarizing the localization of Gas1p in vegetative cells. (A) In a new born cell Gas1p is in microdomains of the plasma membrane. (B) In a small-budded cell, Gas1p is in the plasma membrane but is also linked to the chitin ring presumably through a transglycoylase reaction. (C) In large-budded cells Gas1p is localized to or in close proximity to the primary septum. (D) After mother-daughter separation, Gas1p remains in the bud scar and distributed around the plasma membrane. Another pool of Gas1p probably dispersed all over the cell wall is not indicated. CR, chitin ring; PS, primary septum; BS, bud scar.

of Gas1p fused to GFP used as a marker in studies of lipid rafts polarization (Bagnat and Simons, 2002; Valdez-Taubas and Pelham, 2003).

In a mass spectrometry analysis of the plasma-membrane DRMs, Gas1p, Gas3, Gas5p, and other enzymes involved in cell wall biogenesis, in particular Fks1p/Fks2p, Rho1p, and the GPI-mannoproteins Ecm33p and Crh2p, were identified (Aronova *et al*., 2007). This reinforces the notion that lipid rafts contribute to segregation and sorting membrane districts into which proteins specifically aggregate. A physical association of Gas1p with Fks1p/Fks2p and their regulatory subunit Rho1p could be of functional significance given that these enzymes could cooperate in the synthesis, extrusion and incorporation of β(1,3)-glucans into the expanding cell wall.

Our results confirm and extend previous reports regarding the existence of a cell wall form of Gas1p (De Sampaio *et al*., 1999; Yin *et al*., 2005). We showed that this is not simply a consequence of some leakiness in the mechanism of plasma membrane retention but a specific destination of the protein. A quantitative analysis also revealed that $\sim 6 \times 10^3$ copies of Gas1p per cell are cell wall bound (Yin *et al*., 2007). This corresponds to ~20% of the total Gas1p typically present in a growing yeast cell (Popolo, unpublished data). Thus, the majority of the protein is localized in the plasma membrane but molecular mechanisms must exist to regulate the incorporation of a fraction of Gas1p molecules into the cell wall.

Mechanisms of Incorporation of Gas1 in Specific Sites of the Cell Wall

Evidence that cell wall anchoring of GPI proteins can occur in a selective manner was reported for three structural GPI-mannoproteins, Tip1, Cwp1 and Cwp2 (Smits *et al*., 2006). Cwp1p is localized at the birth scar whereas Tip1p and Cwp2p are incorporated in the mother cells and in small- to medium-sized buds, respectively. The localization of these proteins was shown to be completely determined by the timing of their transcription during the cell cycle (Smits *et al*., 2006). The synthesis of Gas1p is maximal at the G1-to-S transition, which is the moment of chitin ring formation at bud emergence (Popolo *et al*., 1993a; Ram *et al*., 1995). This pattern of expression could also be crucial for the incorporation of Gas1p into the cell wall but other mechanisms cannot be excluded. In fact Crh2p, which is synthesized throughout

the cell cycle, is incorporated in a ring at the base of the bud by a mechanism that depends on actin cytoskeleton and septin ring organization (Rodriguez-Pena *et al*., 2002).

The analyses of purified cell walls from αF-arrested, *crh1*Δ *crh2*Δ and *chs3*Δ cells suggest that Gas1p is present in two pools in growing cells (Supplemental Figure S2). Pool A is represented by a GPI-Gas1p-β(1,6)-glucan complex that is linked to β(1,3)-glucan. This complex is readily extractable by treatment with β(1,3)-glucanase, usually yielding a diffuse band. Moreover this complex is present also in cells with deletions of *CRH* or *CHS3* genes. Pool A is likely to be dispersed all over the cell wall. Pool B is represented by a GPI-Gas1p-β(1,6)-glucan-chitin complex as it is readily released by exochitinase treatment. To identify this new module, we used a pure exochitinase, as the commercial preparation contains proteases that degraded Gas1p. This complex is detected only in cells undergoing the budding cycle. The formation of such a complex requires Chs3-dependent chitin synthesis and Crh enzymes that probably capture the chitin chain during its polymerization and attach it to the β(1,3)-glucan side branch of β(1,6)-glucan linked to Gas1p (Supplemental Figure S2). Based on previous reports this side chain contains one to three glucose residues and is too short to be attacked by β(1,3)-glucanases (Kollar *et al*., 1997). Pool B is further linked to the main β(1,3)-glucan through the reducing end of the β(1,6)-glucan, yielding a form of Gas1p that is simultaneously linked to chitin and β(1,3)-glucan. Our data also suggest that in the bud scars a Pool B-derived structure could be present and be highly resistant to enzymatic extraction. This could be in accordance with the fact that bud scar is an area of the cell wall which remains after the action of hydrolytic enzymes (chitinase and glucanases) involved in cell separation and shows an exceptional stability over time.

Our work provides new evidence on in vivo substrates for Crh1 and Crh2 enzymes. The lack of linkage of Gas1p to the bud neck/bud scars in the *crh1 crh2* null mutant together with the finding that Gas1p was not present in the material released from the cell wall by exochitinase support the notion that these enzymes transfer chitin to the β(1,6)-glucan linked to Gas1p. Thus, Gas1p is the first substrate of Crh1-Crh2 enzymes to be identified.

The lack of Gas1p localization to the chitin ring and its release in the medium in *chs3* null mutants suggests that chitin is necessary for the attachment of the GPI-Gas1p-β(1,6)-glucan complex to the cell wall. As the Gas1p released into the medium in *chs3* cells and also the Gas1p released by exochitinase in wild-type cells have an apparent molecular weight similar to that of GPI-containing Gas1p, we presume that the β(1,6)-glucan is very short. Chemical analysis of the linkage region between Gas1p and β(1,6)-glucan will be required to confirm the connection with the cell wall polysaccharides and characterize the structure of these interconnections.

The chitin made by Chs2p in the septum was shown to be free (Cabib and Duran, 2005). This is in apparent contrast with the Gas1p localization in the primary septum. Although we showed that the Gas1p colocalizes with the chitin of the primary septum, we cannot exclude the possibility that Gas1p is in close proximity to the chitin disk rather than being directly cross-linked to it. Gas1p could be part of the outermost mannoprotein layer of the secondary septa that are in strict contact with the chitin disk. The severe disturbance in the architecture of the septum in the c*hs2* null mutant could be responsible of the release of Gas1p into the medium. Immunoelectron microscopy will be an invaluable technique to investigate the localization of Gas1p in the primary and remedial septa in more detail.

As mentioned in the Introduction, Dfg5p and Dcw1p constitute an essential pair of putative mannosidases and candidates as catalysts of the transfer of the GPI-protein to the β(1,6)-glucan (Kitagaki *et al*., 2002). We found that Gas1p showed the usual locations in single *dfg5*Δ or *dcw1*Δ mutants, indicating that Dfg5p and Dcw1p are not required for the binding of Gas1p to the cell wall (Supplemental Figure S1). However these proteins could contribute to a common function and compensate for each other's absence.

Functional Significance of the Localization of Gas1p in Specific Sites of the Cell Wall

We attempted to elucidate the role of Gas1p at the chitin ring, a special structure in which growth is prevented and resistance must be high to drive the growth into the bud. Several hypotheses can be formulated for the role of Gas1p tethered at the neck region. Gas1p could assume an inactive conformation and prevent incorporation of new β(1,3)-glucan chains in the neck area. It should also be noted that Gas1p is highly glycosylated and contains seven intramolecular disulfide bonds which confer a high stability (Popolo *et al*., 2008). Thus, Gas1p could have a structural role and contribute to the resistance of the neck region and also act as a permeability barrier. Another attractive hypothesis is that Gas1p activity is required for a local remodeling of β(1,3)glucan or for promoting a loosening of the fibers to facilitate, at a later stage, the action of β(1,3)-glucanases, such as Eng1p (Baladron *et al*., 2002).

The availability of a TM-form of Gas1p provided a means to study the functional significance of Gas1p localization in the septum region. By expressing the mRFP-*GAS1-MID2* fusion we could uncouple the functions of GPI-anchored and cell wall-bound Gas1p. We could determine that both forms contribute to bud neck size and facilitate cell separation in agreement with previous observations on the severe defects of *gas1*Δ cells in cell separation (Popolo *et al*., 1993b). As mentioned above, Gas1p is localized at—or in proximity to—the primary septum. Gas1p could be specifically targeted to the cell wall of this region to remodel β(1,3)glucan chains in preparation to cell separation.

Finally, it has been shown that *gas1* null diploid mutants exhibit a random budding pattern (Ni and Snyder, 2001). It is still unclear whether Gas1p in the chitin ring could play an additional role in the marking of the previous budding site. It is also conceivable that the round shape of *gas1* cells could affect the cytoskeleton and be indirectly responsible for the altered budding pattern.

ACKNOWLEDGMENTS

We thank Enrico Cabib, Vladimir Farkas and Javier Arroyo for helpful discussion and strains, Carlos Vazquez de Aldana and Maria de Medina Redondo for critical reading of the manuscript, Roberto Cavatorta for the preparation of the figures, and David Horner for English revision. We thank also Alessandro Nespoli for the assistance in flow cytometry. We are grateful to the National Institute of Advanced Industrial Science and Technology of Japan and Prof. Yoshifumi Jigami for the kind gift of pMF608. This work was partially supported by the European RTN project 512481 "CanTrain" and by the national P.R.I.N. grant 2005 (to L. P.). E. R. is a recipient of a fellowship from Fondo Sociale Europeo 415438. J. C. is a recipient of a Marie Curie contract in the frame of the Cantrain project.

REFERENCES

Aronova, S., Wedaman, K., Anderson, S., Yates, J., 3rd, and Powers, T. (2007). Probing the membrane environment of the TOR kinases reveals functional interactions between TORC1, actin, and membrane trafficking in *Saccharomyces cerevisiae*. Mol. Biol. Cell *18*, 2779–2794.

Bagnat, M., Keranen, S., Shevchenko, A., and Simons, K. (2000). Lipid rafts function in biosynthetic delivery of proteins to the cell surface in yeast. Proc. Natl. Acad. Sci. USA *97*, 3254–3259.

Bagnat, M., and Simons, K. (2002). Lipid rafts in protein sorting and cell polarity in budding yeast *Saccharomyces cerevisiae*. Biol. Chem. *383*, 1475–1480.

Baladron, V., Ufano, S., Duenas, E., Martin-Cuadrado, A. B., del Rey, F., and Vazquez de Aldana, C. R. (2002). Eng1p, an endo-1,3-beta-glucanase localized at the daughter side of the septum, is involved in cell separation in *Saccharomyces cerevisiae*. Eukaryot. Cell *1*, 774–786.

Cabib, E. (2004). The septation apparatus, a chitin-requiring machine in budding yeast. Arch. Biochem. Biophys. *426*, 201–207.

Cabib, E., Blanco, N., Grau, C., Rodriguez-Pena, J. M., and Arroyo, J. (2007). Crh1p and Crh2p are required for the cross-linking of chitin to beta(1-6)glucan in the *Saccharomyces cerevisiae* cell wall. Mol. Microbiol. *63*, 921–935.

Cabib, E., and Duran, A. (2005). Synthase III-dependent chitin is bound to different acceptors depending on location on the cell wall of budding yeast. J. Biol. Chem. *280*, 9170–9179.

Cabib, E., Farkas, V., Kosik, O., Blanco, N., Arroyo, J., and McPhie, P. (2008). Assembly of the yeast cell wall. Crh1p and Crh2p act as transglycosylases in vivo and in vitro. J. Biol. Chem. *283*, 29859–29872.

Cabib, E., Sburlati, A., Bowers, B., and Silverman, S. J. (1989). Chitin synthase 1, an auxiliary enzyme for chitin synthesis in *Saccharomyces cerevisiae*. J. Cell Biol. *108*, 1665–1672.

Cabib, E., and Schmidt, M. (2003). Chitin synthase III activity, but not the chitin ring, is required for remedial septa formation in budding yeast. FEMS Microbiol. Lett. *224*, 299–305.

Carotti, C., Ragni, E., Palomares, O., Fontane, T., Tedeschi, G., Rodriguez, R., Latgé, J. P., Vai, M., and Popolo, L. (2004). Characterization of recombinant forms of the yeast Gas protein and identification of residues essential for glucanosyltransferase activity and folding. Eur. J. Biochem. *271*, 3635–3645.

de Groot, P. W., de Boer, A. D., Cunningham, J., Dekker, H. L., de Jong, L., Hellingwerf, K. J., de Koster, C., and Klis, F. M. (2004). Proteomic analysis of Candida albicans cell walls reveals covalently bound carbohydrate-active enzymes and adhesins. Eukaryot. Cell *3*, 955–965.

De Sampaio, G., Bourdineaud, J. P., and Lauquin, G. J. (1999). A constitutive role for GPI anchors in *Saccharomyces cerevisiae*: cell wall targeting. Mol. Microbiol. *34*, 247–256.

Fujita, M., Yoko, O. T., and Jigami, Y. (2006). Inositol deacylation by Bst1p is required for the quality control of glycosylphosphatidylinositol-anchored proteins. Mol. Biol. Cell *17*, 834–850.

Gatti, E., Popolo, L., Vai, M., Rota, N., and Alberghina, L. (1994). O-linked oligosaccharides in yeast glycosyl phosphatidylinositol-anchored protein gp115 are clustered in a serine-rich region not essential for its function. J. Biol. Chem. *269*, 19695–19700.

Kitagaki, H., Wu, H., Shimoi, H., and Ito, K. (2002). Two homologous genes, DCW1 (YKL046c) and DFG5, are essential for cell growth and encode glycosylphosphatidylinositol (GPI)-anchored membrane proteins required for cell wall biogenesis in *Saccharomyces cerevisiae*. Mol. Microbiol. *46*, 1011–1022.

Klis, F. M., Boorsma, A., and De Groot, P. W. (2006). Cell wall construction in *Saccharomyces cerevisiae*. Yeast *23*, 185–202.

Kollar, R., Petrakova, E., Ashwell, G., Robbins, P. W., and Cabib, E. (1995). Architecture of the yeast cell wall. The linkage between chitin and beta(1->3)-glucan. J. Biol. Chem. *270*, 1170–1178.

Kollar, R., Reinhold, B. B., Petrakova, E., Yeh, H. J., Ashwell, G., Drgonova, J., Kapteyn, J. C., Klis, F. M., and Cabib, E. (1997). Architecture of the yeast cell wall. Beta(1->6)-glucan interconnects mannoprotein, beta(1->)3-glucan, and chitin. J. Biol. Chem. *272*, 17762–17775.

Lesage, G., and Bussey, H. (2006). Cell wall assembly in *Saccharomyces cerevisiae*. Microbiol. Mol. Biol. Rev. *70*, 317–343.

Lesage, G., Sdicu, A. M., Menard, P., Shapiro, J., Hussein, S., and Bussey, H. (2004). Analysis of beta-1,3-glucan assembly in *Saccharomyces cerevisiae* using a synthetic interaction network and altered sensitivity to caspofungin. Genetics *167*, 35–49.

Malinska, K., Malinsky, J., Opekarova, M., and Tanner, W. (2004). Distribution of Can1p into stable domains reflects lateral protein segregation within the plasma membrane of living *S. cerevisiae* cells. J. Cell Sci. *117*, 6031–6041.

Montijn, R. C., Vink, E., Muller, W. H., Verkleij, A. J., Van Den Ende, H., Henrissat, B., and Klis, F. M. (1999). Localization of synthesis of beta1,6-glucan in *Saccharomyces cerevisiae*. J. Bacteriol. *181*, 7414–7420.

Mouyna, I., Fontaine, T., Vai, M., Monod, M., Fonzi, W. A., Diaquin, M., Popolo, L., Hartland, R. P., and Latge, J. P. (2000). Glycosylphosphatidylinositol-anchored glucanosyltransferases play an active role in the biosynthesis of the fungal cell wall. J. Biol. Chem. *275*, 14882–14889.

Ni, L., and Snyder, M. (2001). A genomic study of the bipolar bud site selection pattern in *Saccharomyces cerevisiae*. Mol. Biol. Cell *12*, 2147–2170.

Popolo, L., Cavadini, P., Vai, M., and Alberghina, L. (1993a). Transcript accumulation of the GGP1 gene, encoding a yeast GPI-anchored glycoprotein, is inhibited during arrest in the G1 phase and during sporulation. Curr. Genet. *24*, 382–387.

Popolo, L., Gilardelli, D., Bonfante, P., and Vai, M. (1997). Increase in chitin as an essential response to defects in assembly of cell wall polymers in the ggp1delta mutant of *Saccharomyces cerevisiae*. J. Bacteriol. *179*, 463–469.

Popolo, L., Ragni, E., Carotti, C., Palomares, O., Aardema, R., Back, J. W., Dekker, H. L., de Koning, L. J., de Jong, L., and de Koster, C. G. (2008). Disulfide bond structure and domain organization of yeast β(1,3)-glucanosyltransferases involved in cell wall biogenesis. J. Biol. Chem. *283*, 18553–18565.

Popolo, L., and Vai, M. (1999). The Gas1 glycoprotein, a putative wall polymer cross-linker. Biochim. Biophys. Acta *1426*, 385–400.

Popolo, L., Vai, M., Gatti, E., Porello, S., Bonfante, P., Balestrini, R., and Alberghina, L. (1993b). Physiological analysis of mutants indicates involvement of the *Saccharomyces cerevisiae* GPI-anchored protein gp115 in morphogenesis and cell separation. J. Bacteriol. *175*, 1879–1885.

Primig, M., Williams, R. M., Winzeler, E. A., Tevzadze, G. G., Conway, A. R., Hwang, S. Y., Davis, R. W., and Esposito, R. E. (2000). The core meiotic transcriptome in budding yeasts. Nat. Genet. *26*, 415–423.

Ragni, E., Coluccio, A., Rolli, E., Rodriguez-Pena, J. M., Colasante, G., Arroyo, J., Neiman, A. M., and Popolo, L. (2007a). GAS2 and GAS4, a pair of developmentally regulated genes required for spore wall assembly in *Saccharomyces cerevisiae*. Eukaryot. Cell *6*, 302–316.

Ragni, E., Fontaine, T., Gissi, C., Latge, J. P., and Popolo, L. (2007b). The Gas family of proteins of *Saccharomyces cerevisiae*: characterization and evolutionary analysis. Yeast *24*, 297–308.

Ram, A. F., Brekelmans, S. S., Oehlen, L. J., and Klis, F. M. (1995). Identification of two cell cycle regulated genes affecting the beta 1,3-glucan content of cell walls in *Saccharomyces cerevisiae*. FEBS Lett. *358*, 165–170.

Rodriguez-Pena, J. M., Rodriguez, C., Alvarez, A., Nombela, C., and Arroyo, J. (2002). Mechanisms for targeting of the *Saccharomyces cerevisiae* GPI-anchored cell wall protein Crh2p to polarised growth sites. J. Cell Sci. *115*, 2549–2558.

Schmidt, M., Varma, A., Drgon, T., Bowers, B., and Cabib, E. (2003). Septins, under Cla4p regulation, and the chitin ring are required for neck integrity in budding yeast. Mol. Biol. Cell *14*, 2128–2141.

Shaw, J. A., Mol, P. C., Bowers, B., Silverman, S. J., Valdivieso, M. H., Duran, A., and Cabib, E. (1991). The function of chitin synthases 2 and 3 in the *Saccharomyces cerevisiae* cell cycle. J. Cell Biol. *114*, 111–123.

Simons, K., and Vaz, W. L. (2004). Model systems, lipid rafts, and cell membranes. Annu. Rev. Biophys. Biomol. Struct. *33*, 269–295.

Smits, G. J., Schenkman, L. R., Brul, S., Pringle, J. R., and Klis, F. M. (2006). Role of cell cycle-regulated expression in the localized incorporation of cell wall proteins in yeast. Mol. Biol. Cell *17*, 3267–3280.

Straede, A., and Heinisch, J. J. (2007). Functional analyses of the extra- and intracellular domains of the yeast cell wall integrity sensors Mid2 and Wsc1. FEBS Lett. *581*, 4495–4500.

Vai, M., Gatti, E., Lacana, E., Popolo, L., and Alberghina, L. (1991). Isolation and deduced amino acid sequence of the gene encoding gp115, a yeast glycophospholipid-anchored protein containing a serine-rich region. J. Biol. Chem. *266*, 12242–12248.

Valdez-Taubas, J., and Pelham, H. R. (2003). Slow diffusion of proteins in the yeast plasma membrane allows polarity to be maintained by endocytic cycling. Curr. Biol. *13*, 1636–1640.

Valdivieso, M. H., Ferrario, L., Vai, M., Duran, A., and Popolo, L. (2000). Chitin synthesis in a gas1 mutant of *Saccharomyces cerevisiae*. J. Bacteriol. *182*, 4752–4757.

Warenda, A. J., and Konopka, J. B. (2002). Septin function in Candida albicans morphogenesis. Mol. Biol. Cell *13*, 2732–2746.

Yin, Q. Y., de Groot, P. W., de Jong, L., Klis, F. M., and De Koster, C. G. (2007). Mass spectrometric quantitation of covalently bound cell wall proteins in *Saccharomyces cerevisiae*. FEMS Yeast Res. *7*, 887–896.

Yin, Q. Y., de Groot, P. W., Dekker, H. L., de Jong, L., Klis, F. M., and de Koster, C. G. (2005). Comprehensive proteomic analysis of *Saccharomyces cerevisiae* cell walls: identification of proteins covalently attached via glycosylphosphatidylinositol remnants or mild alkali-sensitive linkages. J. Biol. Chem. *280*, 20894–20901.